# Cosmology

## and Large Scale Structure

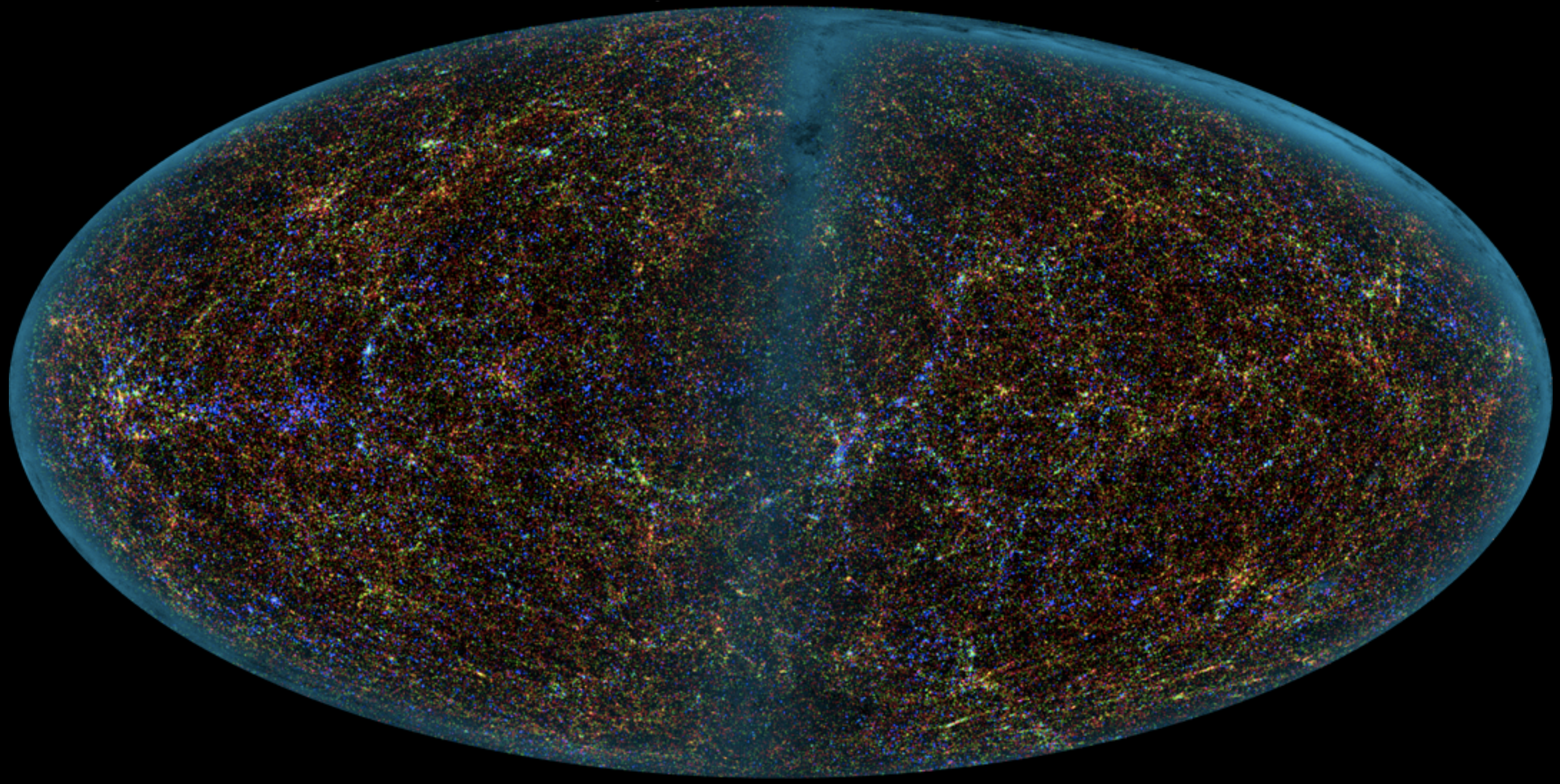

Today

Observational Tests

Galaxy evolution
k-corrections

27 September 2022

http://astroweb.case.edu/ssm/ASTR328/

# What We Need

- Stellar theory predicts the evolution or (***stellar tracks***) or stars of a given mass. There is some variation among different theoretical models
- Observations give us ***libraries of stellar spectra*** as a function of age, mass, metallicity, etc.
- We need the ***initial mass function (IMF)*** of stars
- All of these are uncertain at very low metallicities and high stellar masses
- We have to assume some ***star formation rate (SFR)*** as a function of time. Popular choices include a sharp burst, a constant SFR, or an exponentially declining one:

$$\frac{\partial M}{\partial t} \propto \exp\left(-\frac{t}{\tau}\right)$$

Djorgovski (2017)

# Galaxy Evolution

**SSP**: evolution of simple stellar population in which all stars are born at the same time.

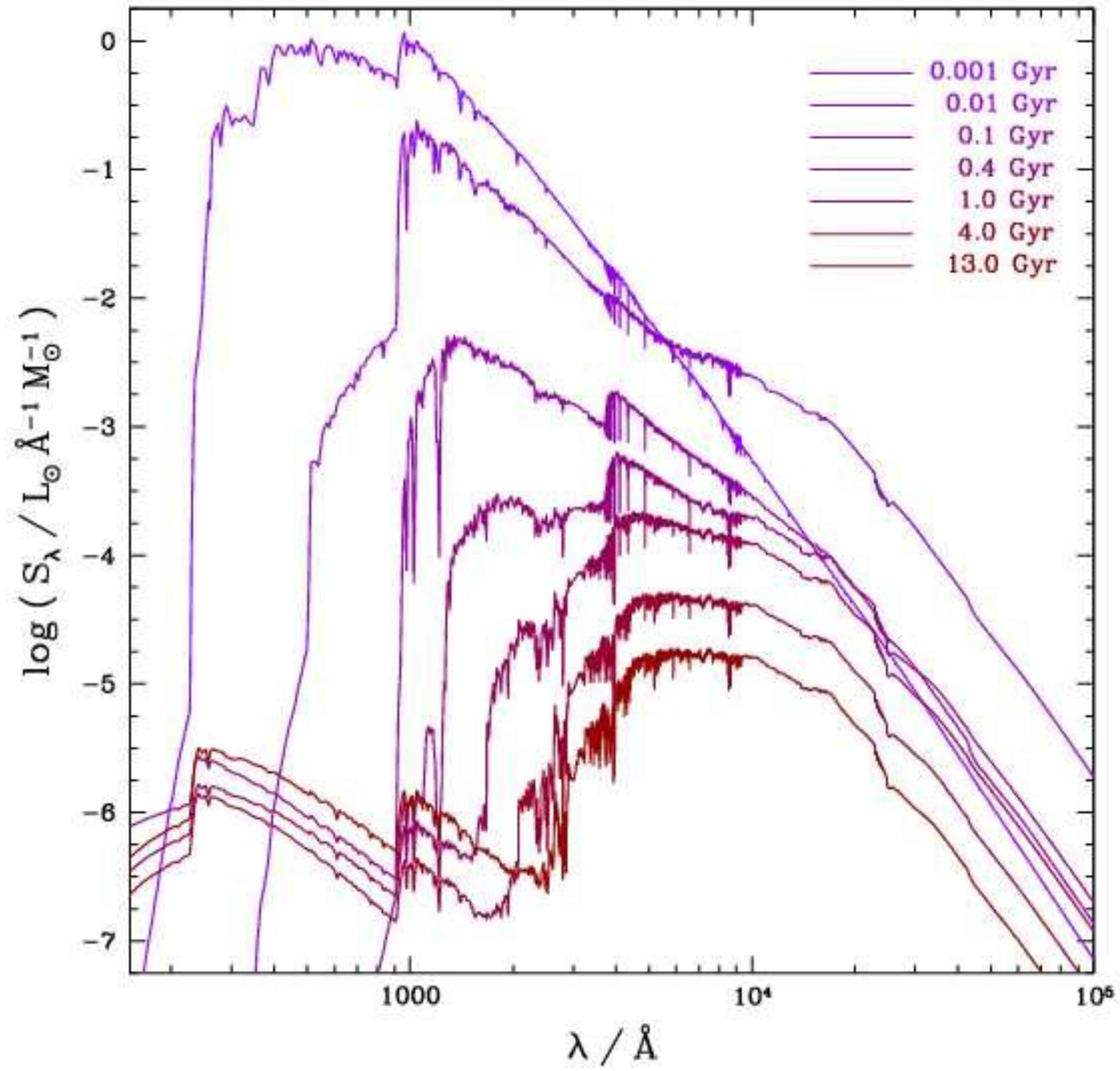


**IMF**
(distribution of stellar masses at birth)

**Stellar Evolution**

**Stellar Spectra**

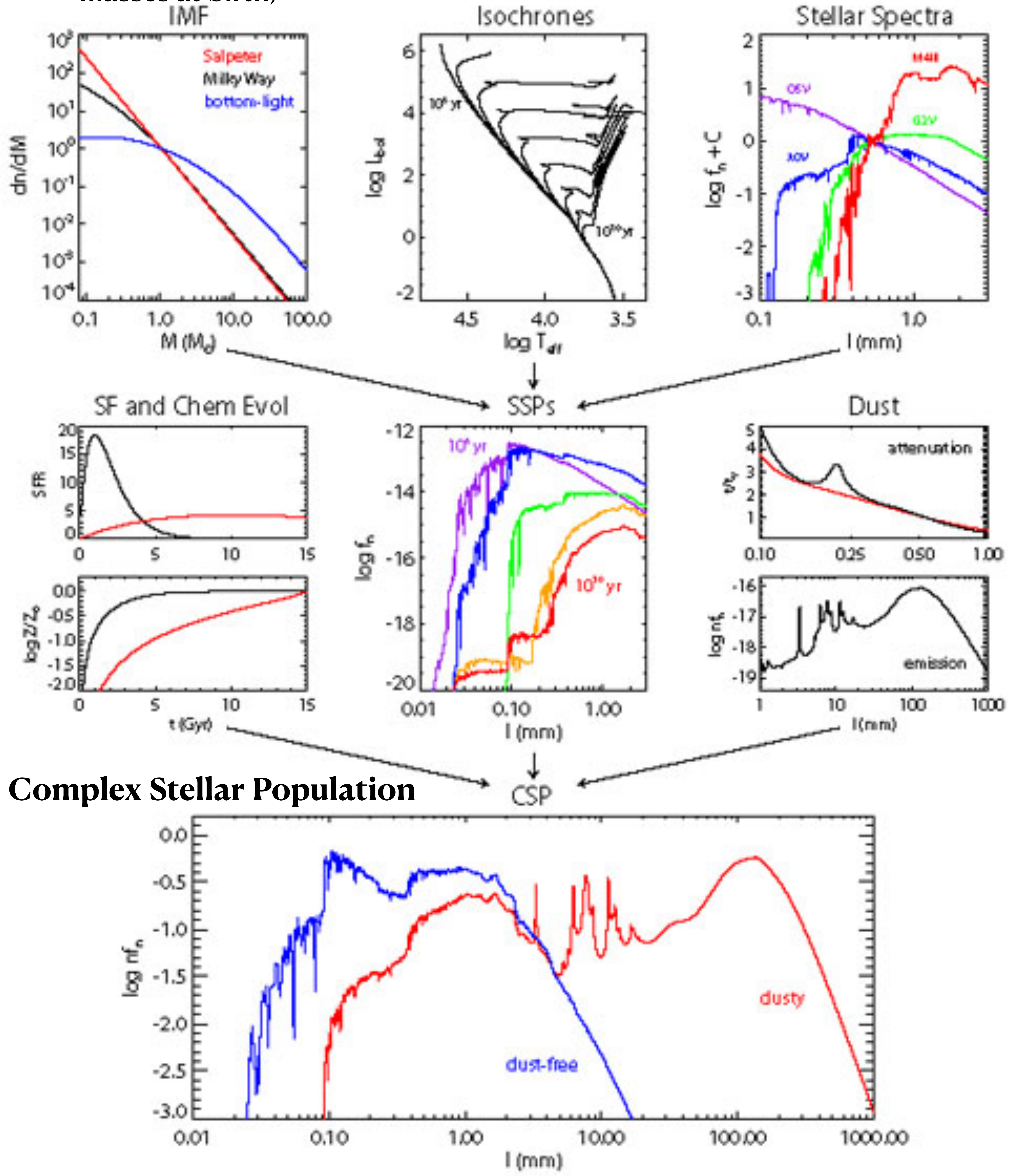

# Galaxy Evolution

Early Types
(Ellipticals)

**Star formation rate**

Sandage (1986)

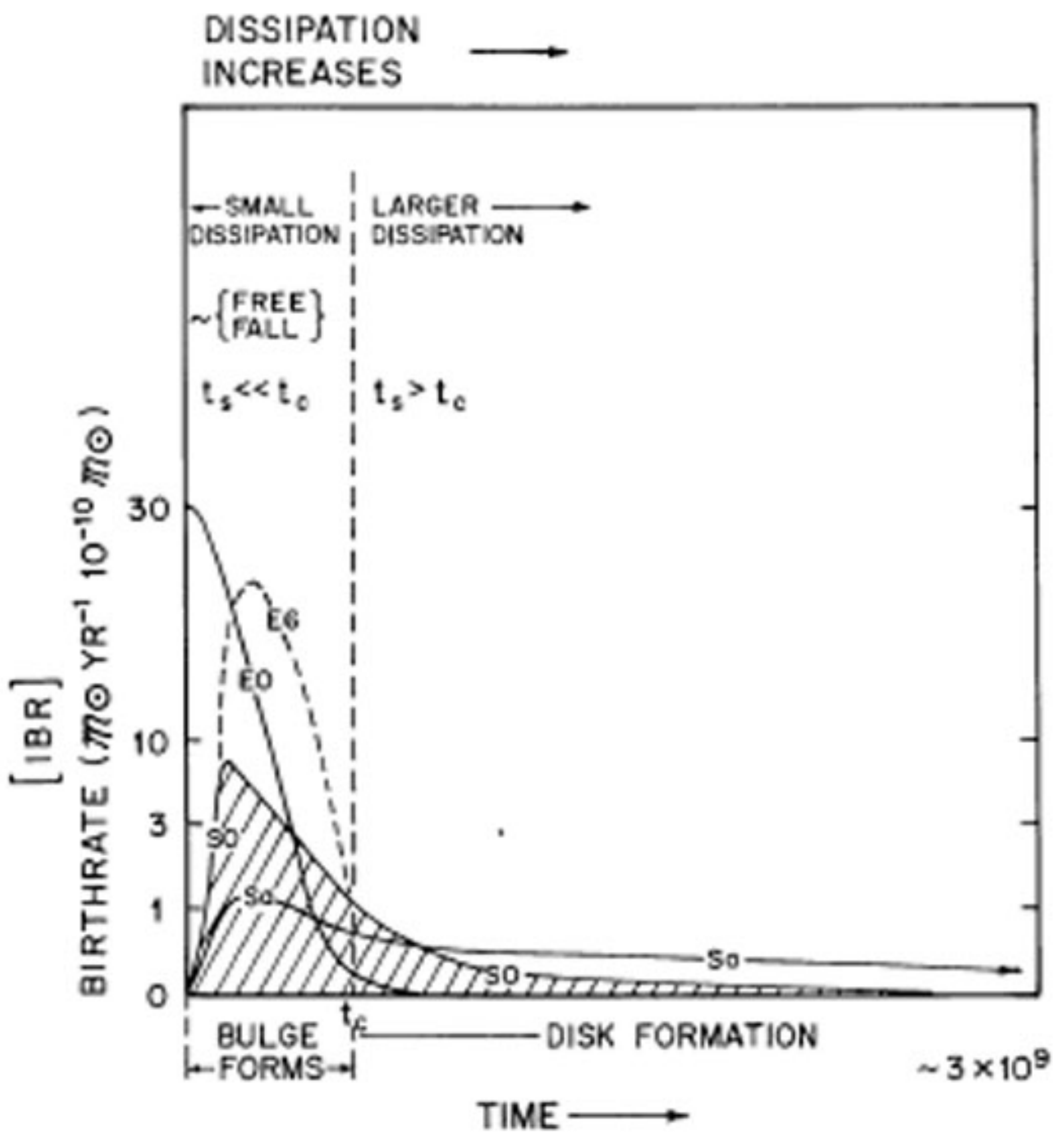


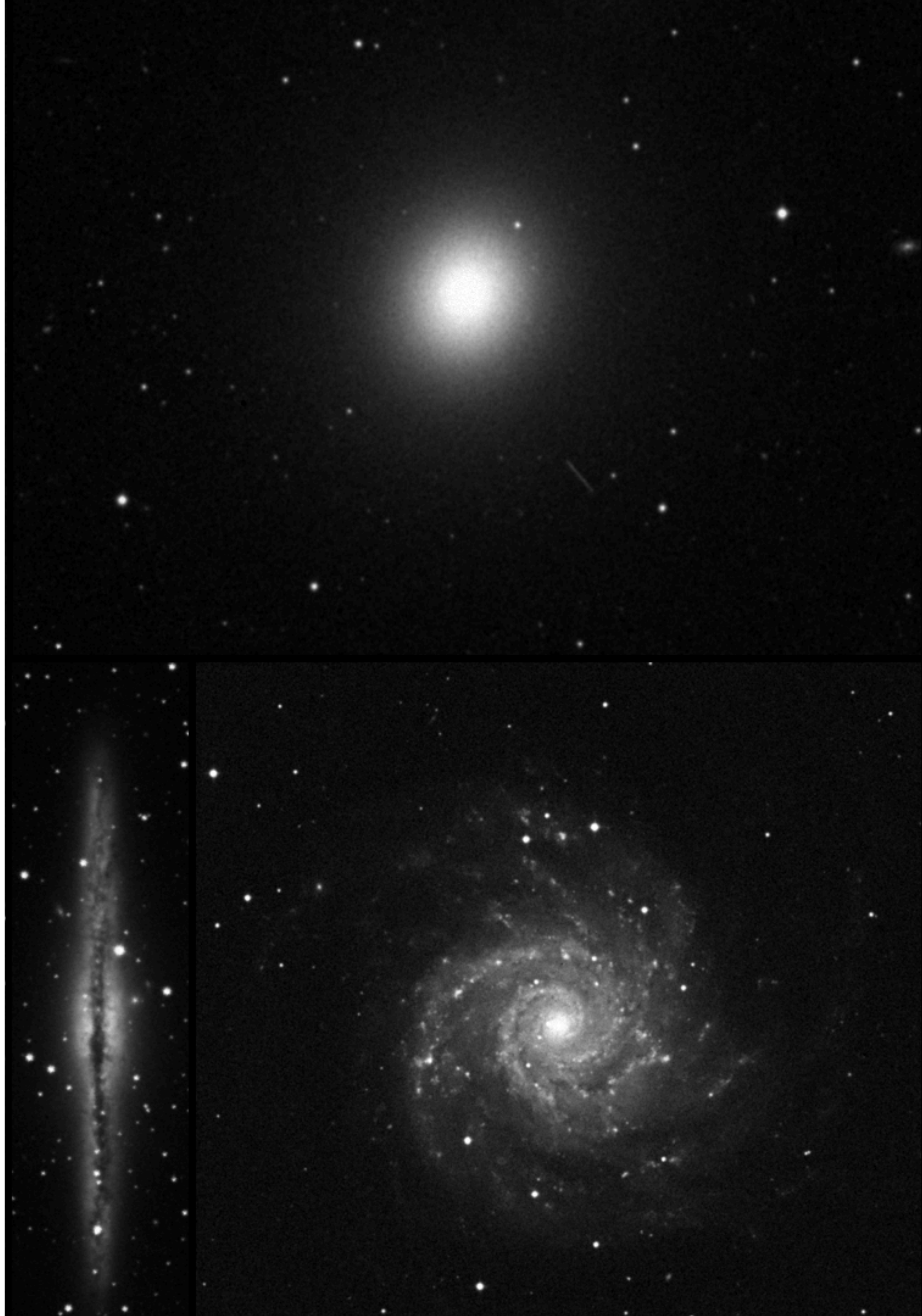

Late Types
(Spirals & Irregulars)

# Galaxy Evolution

Early Type Galaxies (aka ETGs: Elliptical galaxies) generally formed most their stars early, in the first few billion years or so.

Late Types (aka LTGs: Spirals & Irregular galaxies) have a more continuous star formation history, and continue to form stars today.

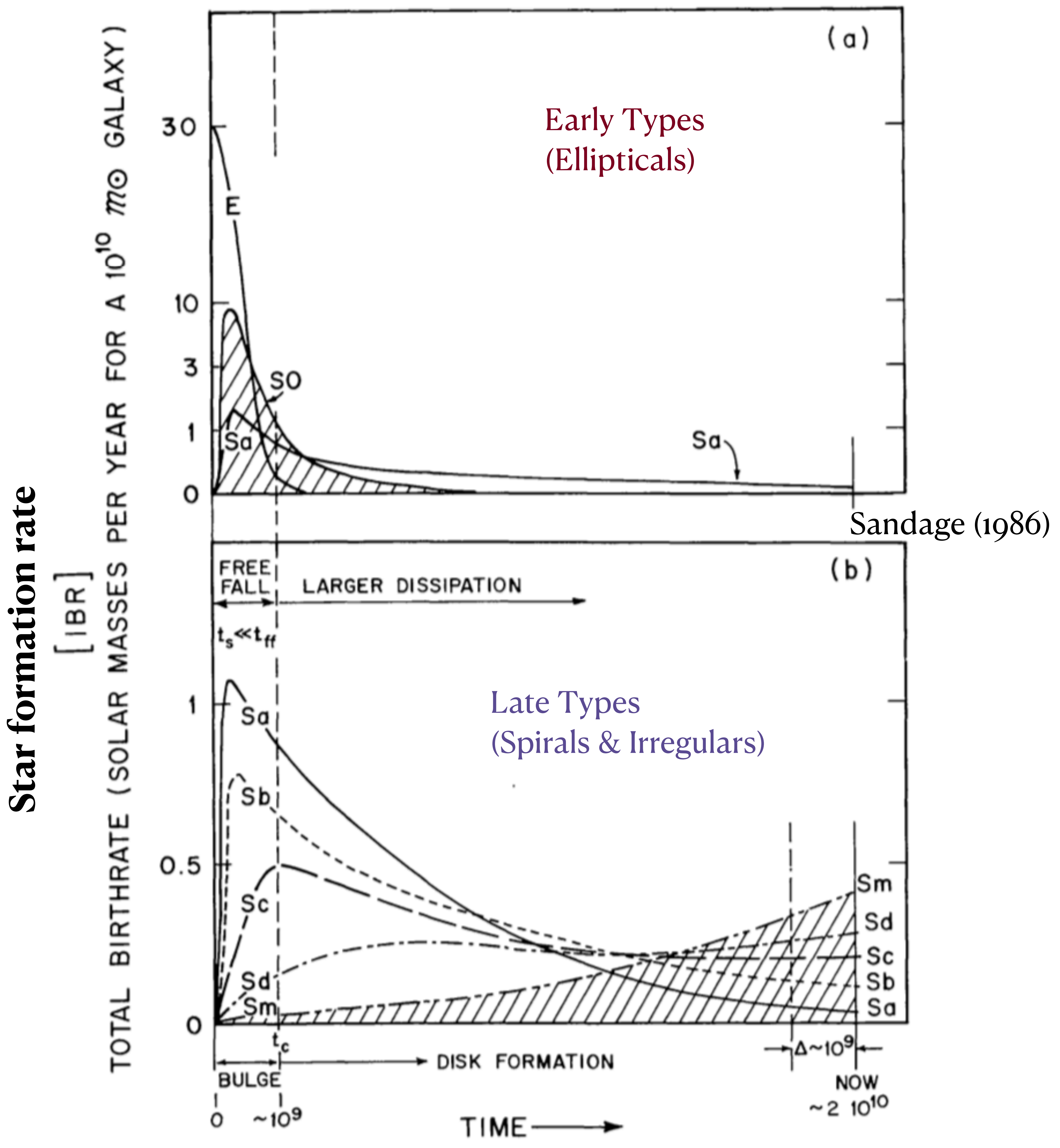


**Fig. 10.** Same as Fig. 9 with later Hubble types shown in the lower panel. The integral under the Sm curve is shaded for illustration. The curves are only schematic showing the trends that have been established by Gallagher et al. (1984)

# Galaxy Evolution

Common model star formation history

Exponential:

$$\mathrm{SFR} = \dot{M}_* = \Psi(t, T) \propto e^{-t/\tau}$$

with different e-folding timescales characteristic of different morphological types $T$.

ETGs typically have small $\tau \approx 1$ Gyr;
LTGs typically have longer timescales, sometimes of order a Hubble time.
Individual galaxies vary substantially.

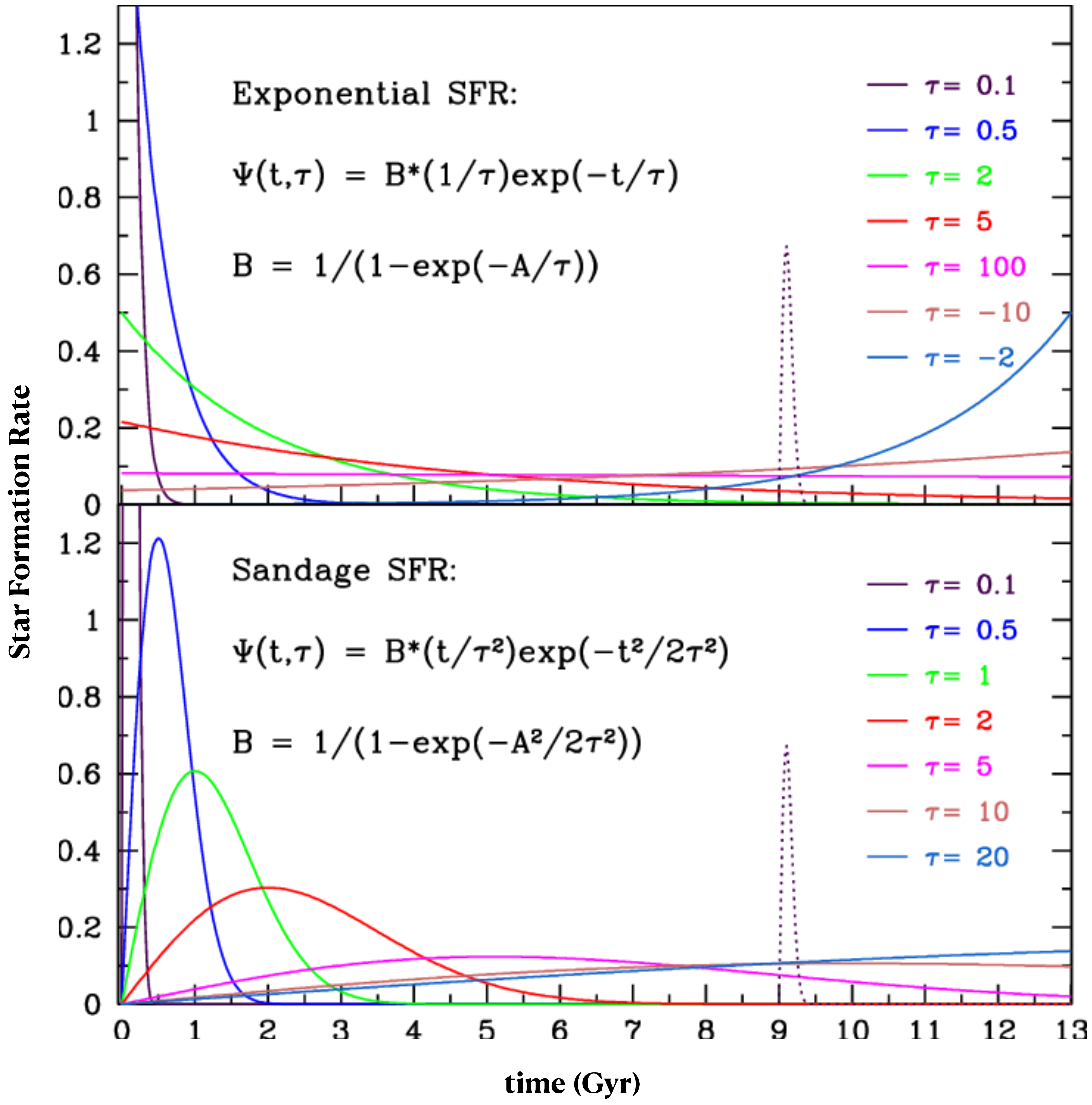

## Star formation and Stellar mass - the "star forming main sequence"

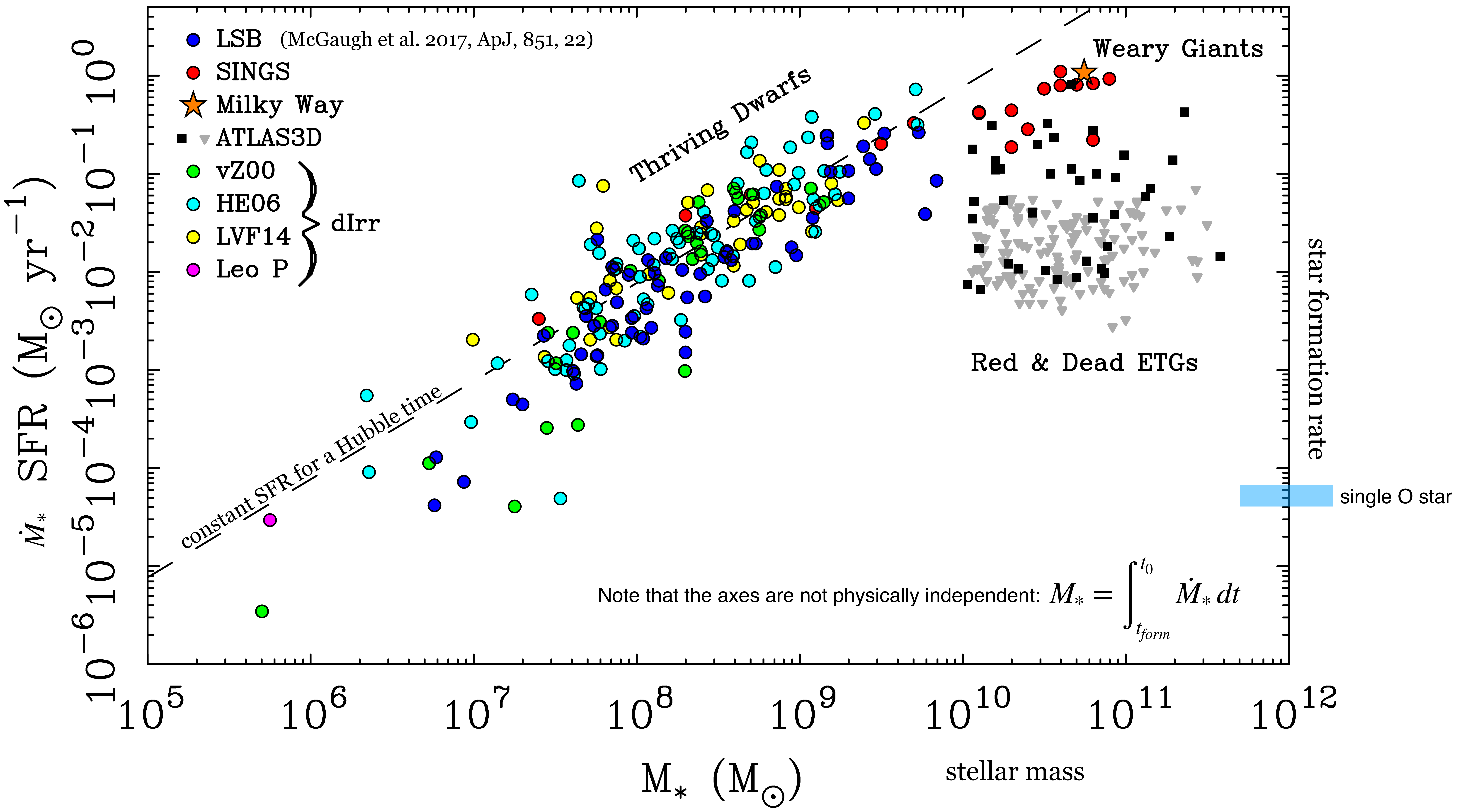

# Galaxy Evolution

ETGs typically have small $\tau \approx 1$ Gyr;
LTGs typically have longer timescales,
often roughly constant but usually with
substantial short-term variations.

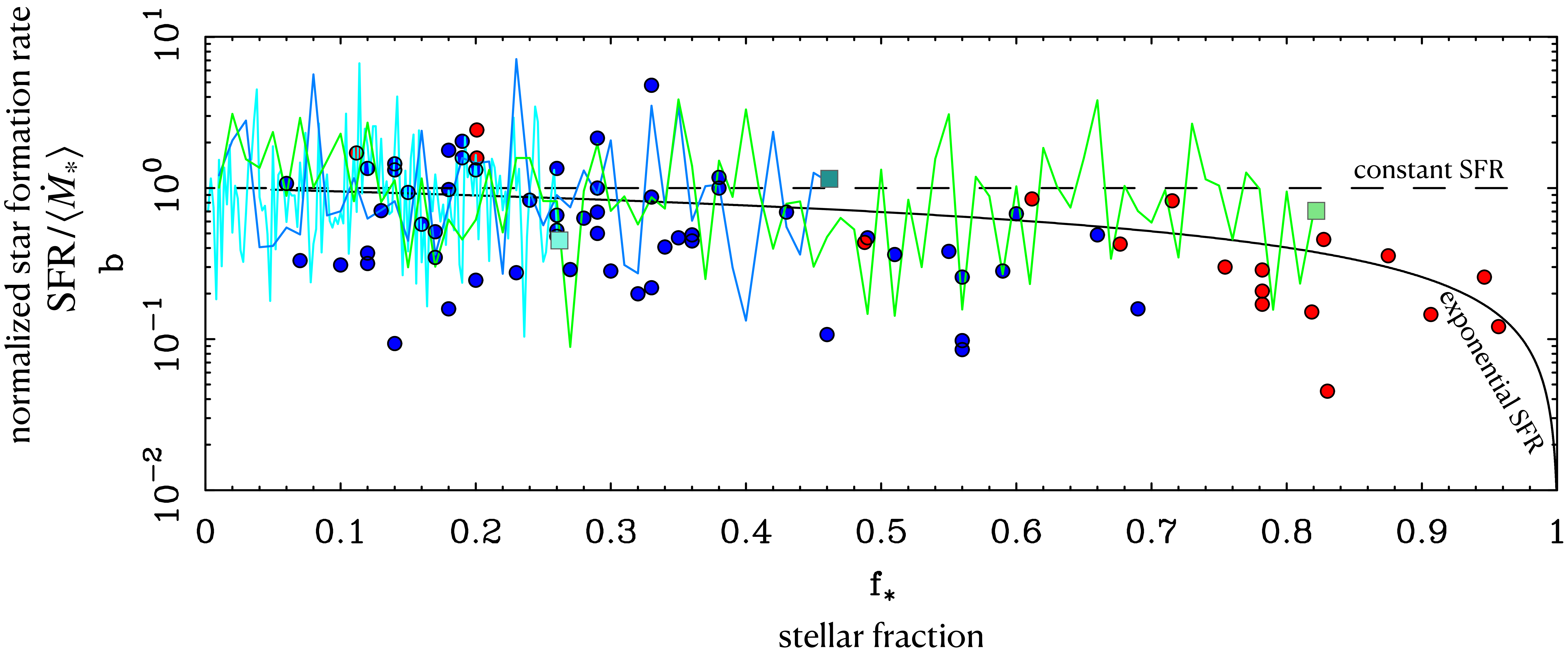


$$b = \frac{\dot{M}_*}{\int_0^t \dot{M}_*\, dt} = \frac{\dot{M}_*}{\langle \dot{M}_* \rangle} \approx \frac{\mathrm{SFR}}{M_*/t}$$

$$f_* = \frac{M_*}{M_* + M_g}$$

# Gas mass and Stellar mass

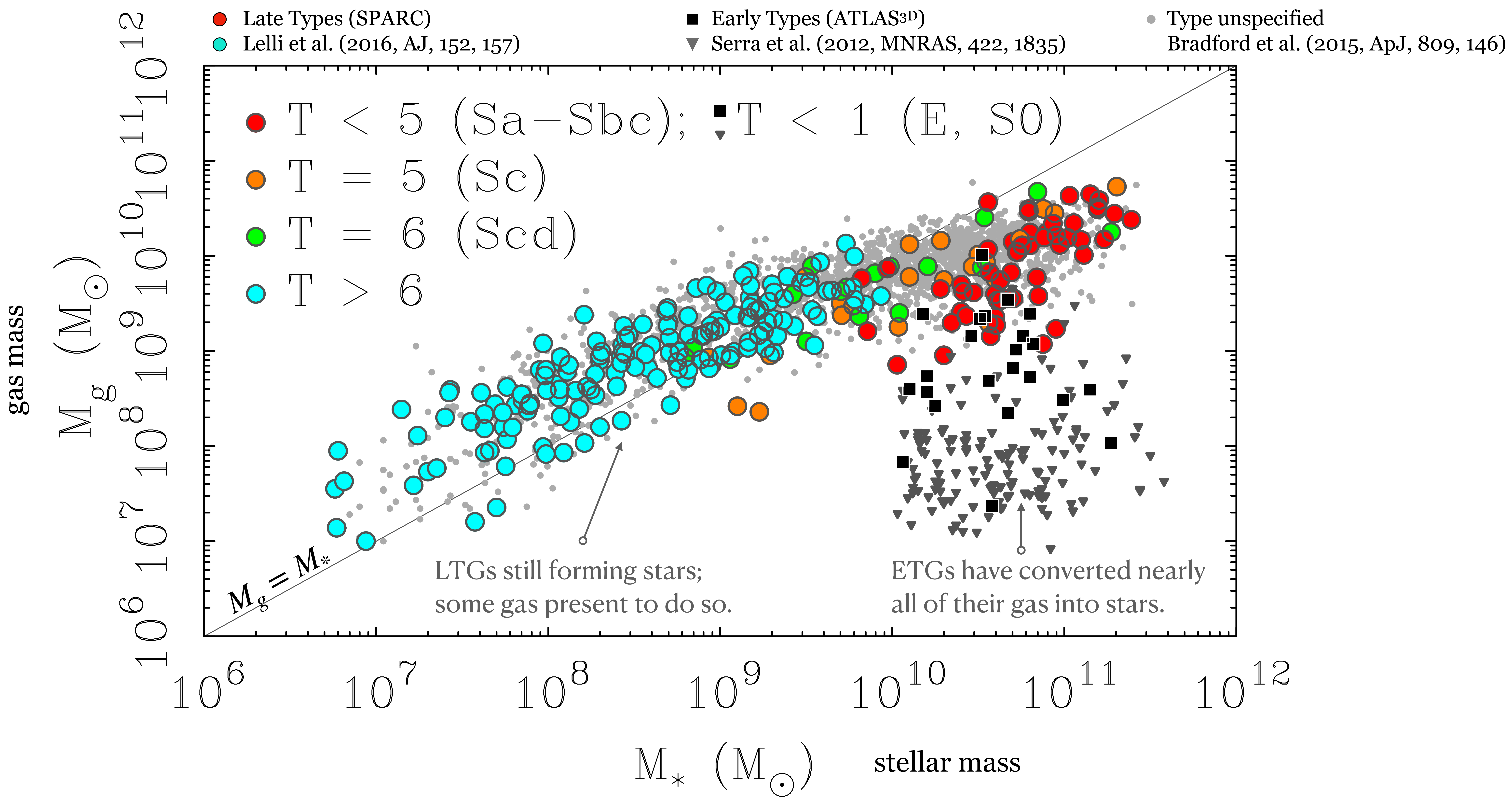

## Integrated stellar mass and star formation rate

$$\rho_* = \int_0^t \psi dt'$$

stellar mass density

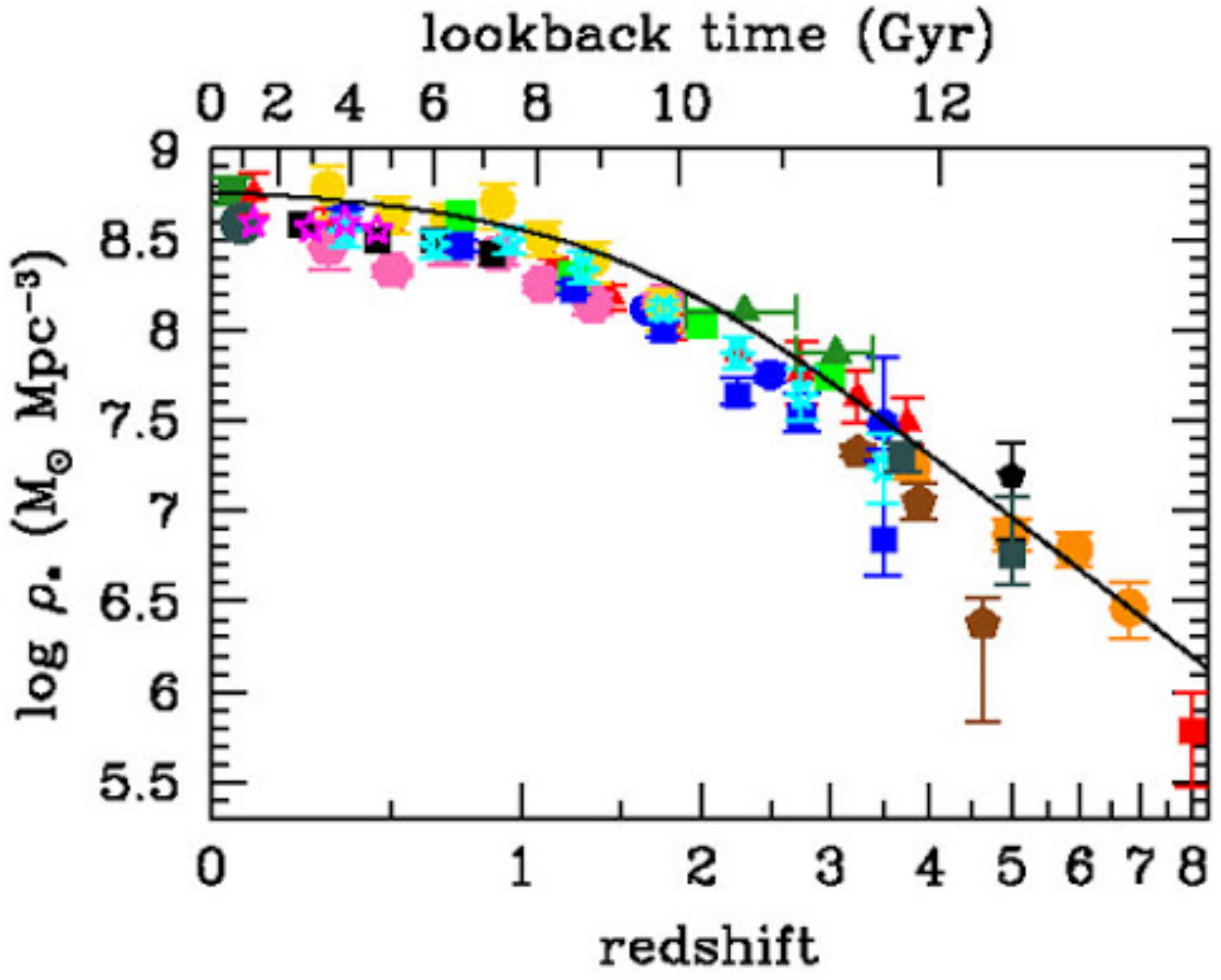


star formation rate

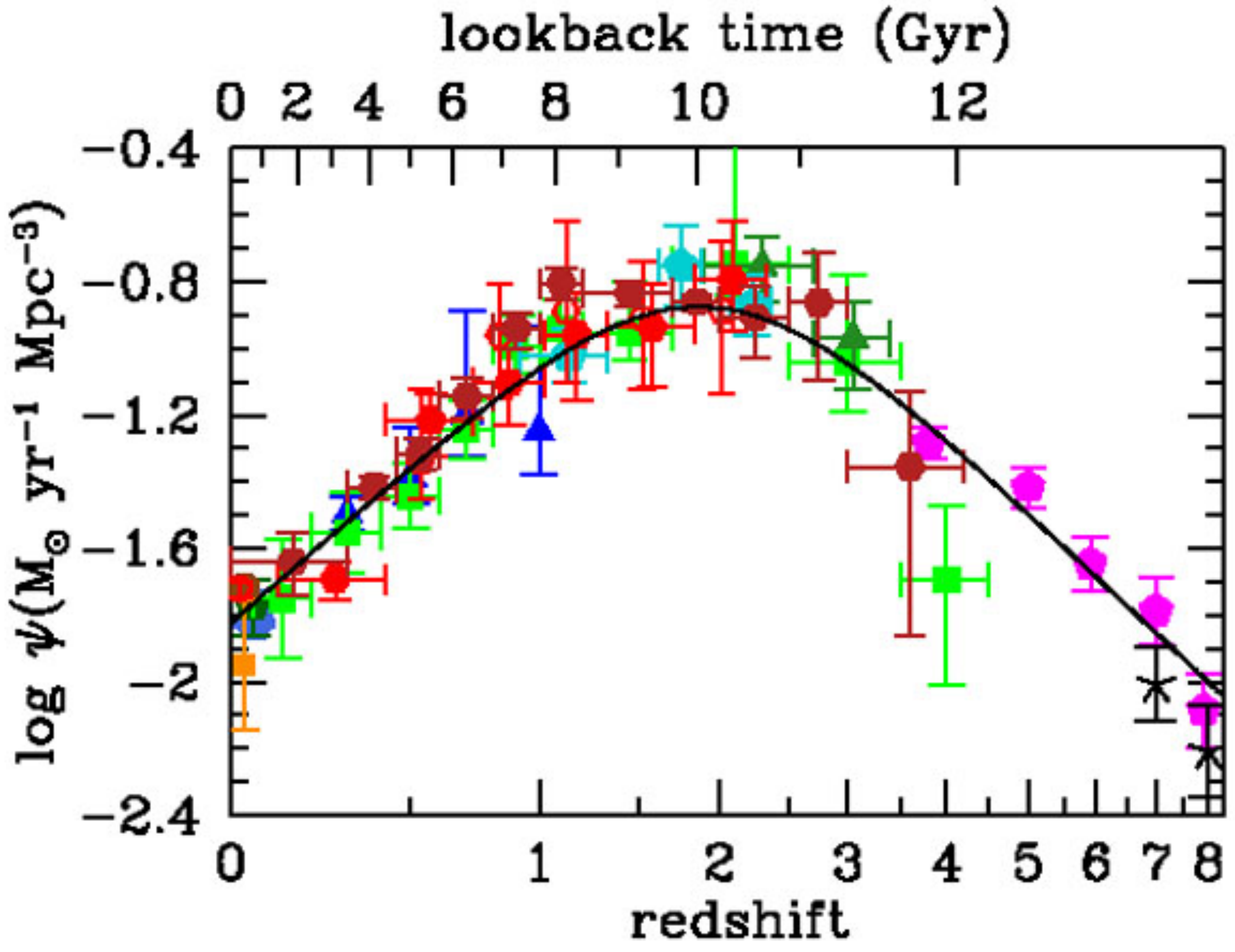


The mass density in stars is small: about 7% of the BBN baryon density

$$\Omega_{*_0} \approx 0.0035$$

$$\Omega_{*_0} = \Upsilon_*[\Phi_0^* L_0^* \Gamma(\alpha)]/\rho_c$$

Stellar mass-to-light ratio

Schechter function at $z = 0$

critical density

The cosmic star formation rate peaked early, around $z \approx 2$ (about 10 Gyr ago).

The star formation rate at high redshift is highly uncertain due to extinction corrections.

# Schechter function fit to data at $z \approx 3$

Franck & McGaugh (2017)

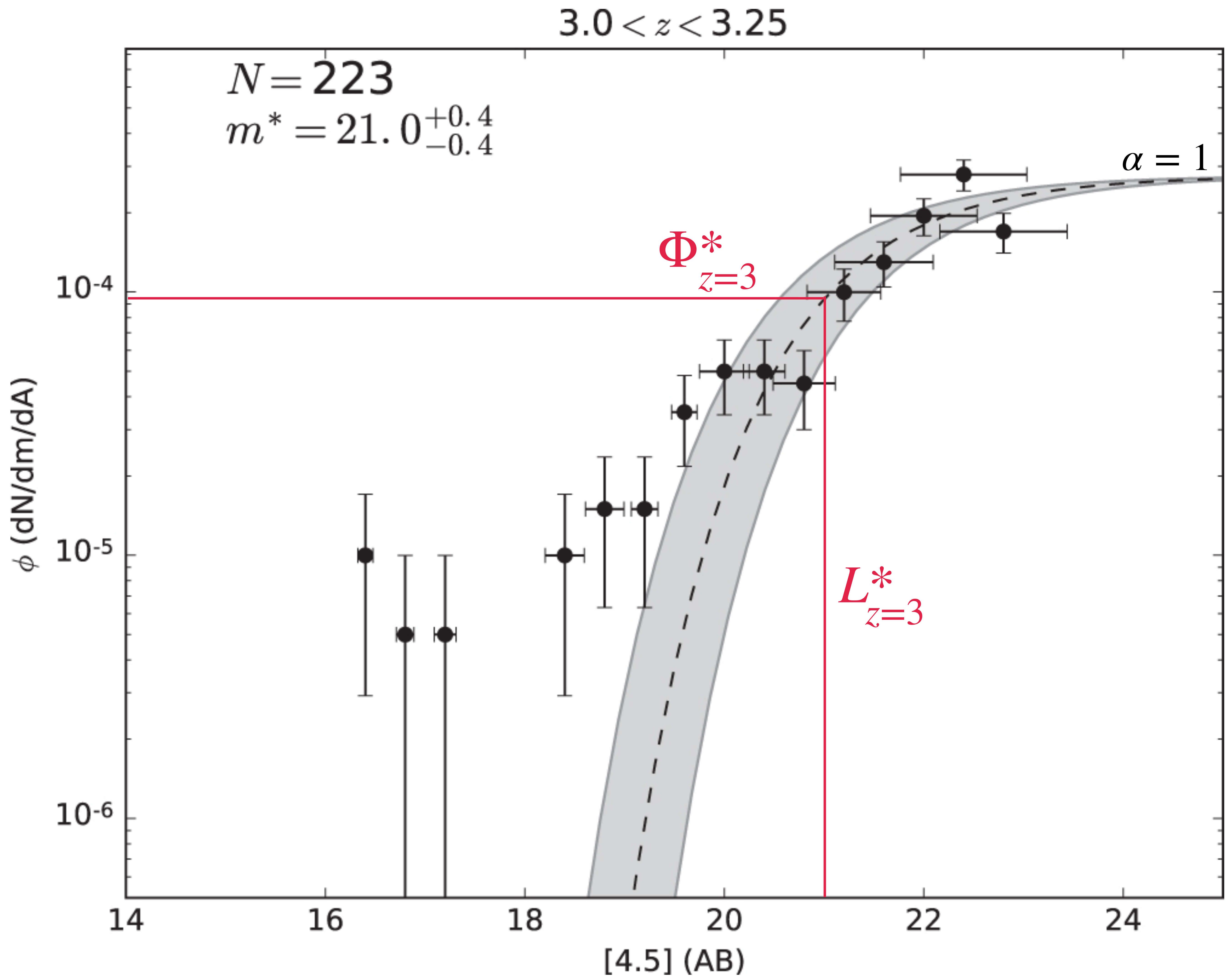

# Schechter fits to data in different redshift bins

McLeod (arXiv: 2009.03176)

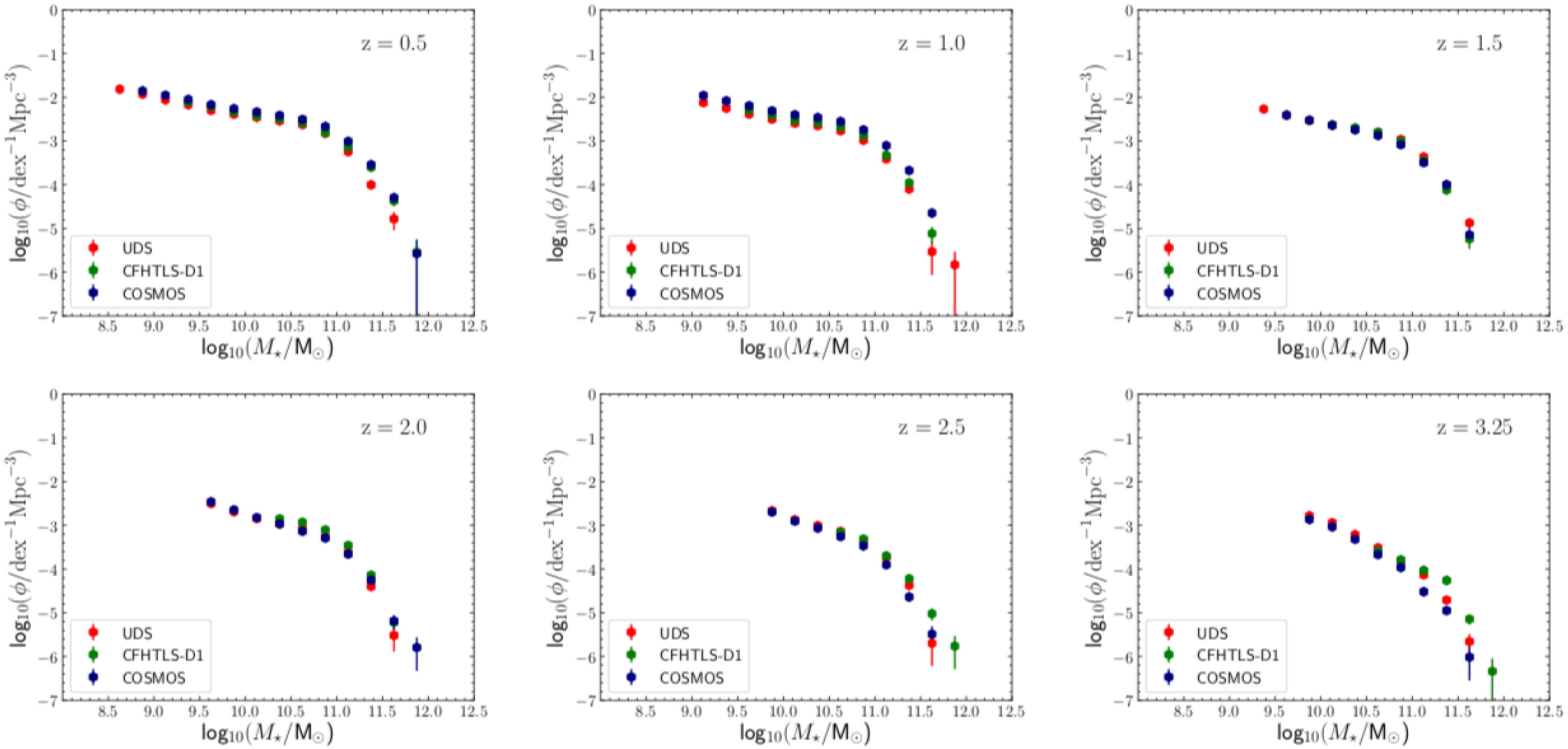


**Figure 3.** A comparison of how the observed GSMF evolves as a function of redshift in our three, degree-scale, survey fields. In this plot the number density uncertainties are simply the Poissonian counting errors. The availability of three, non-contiguous, degree-scale survey fields allows an empirical measurement of the level of cosmic variance in the high-mass end of the GSMF (see text for discussion).

Note that the shape of the luminosity function evolves; the knee only appears around $z \sim 2$

Stefanon+ (2021)

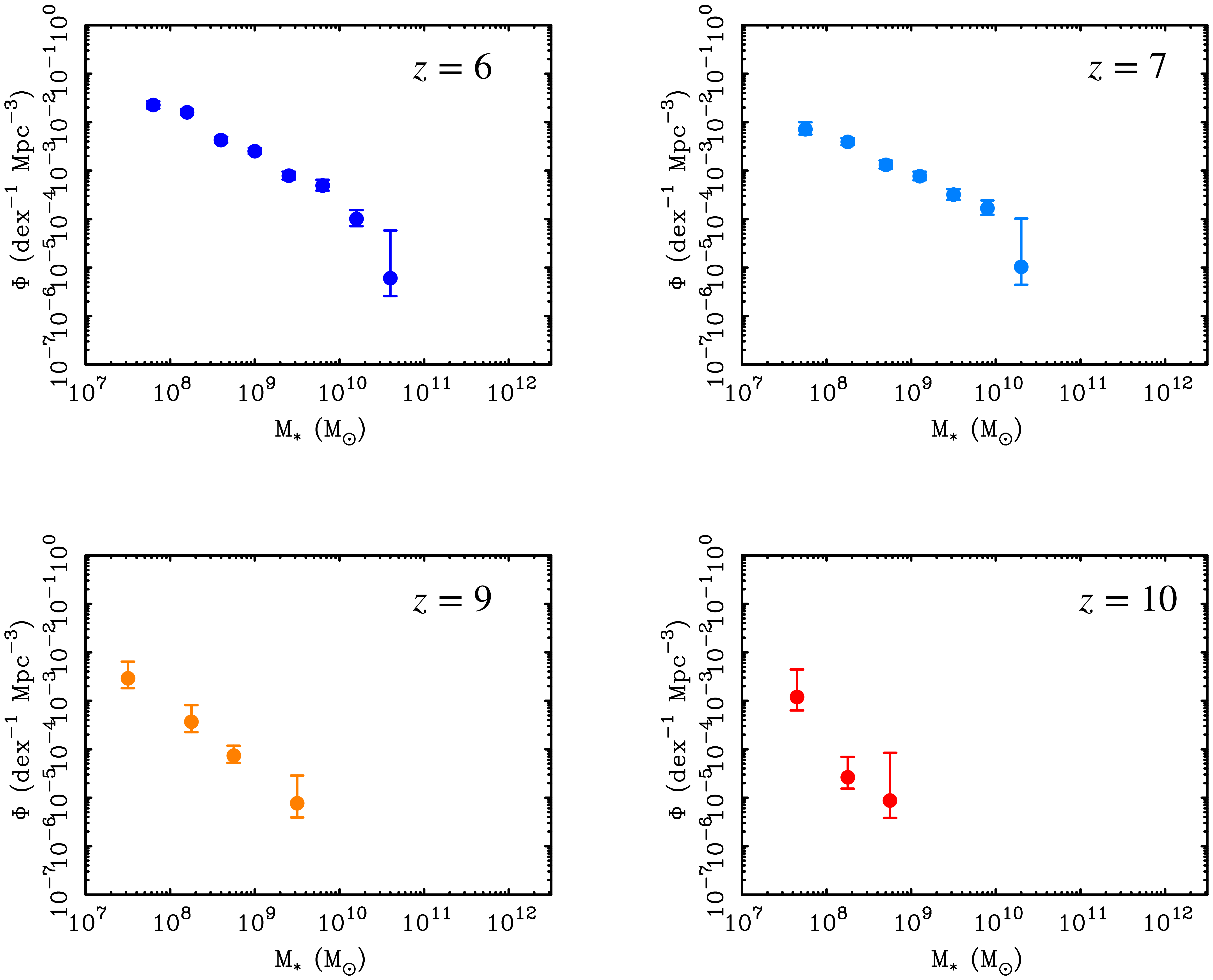


To measure the luminosity function, we have to estimate the volume surveyed, which means assuming a cosmology to compute $d_L$ and $V(z)$.

The luminosity function evolves; galaxies are fainter and the knee disappears at high redshift

Cosmic background radiation: photon energy at all wavelengths over the whole sky

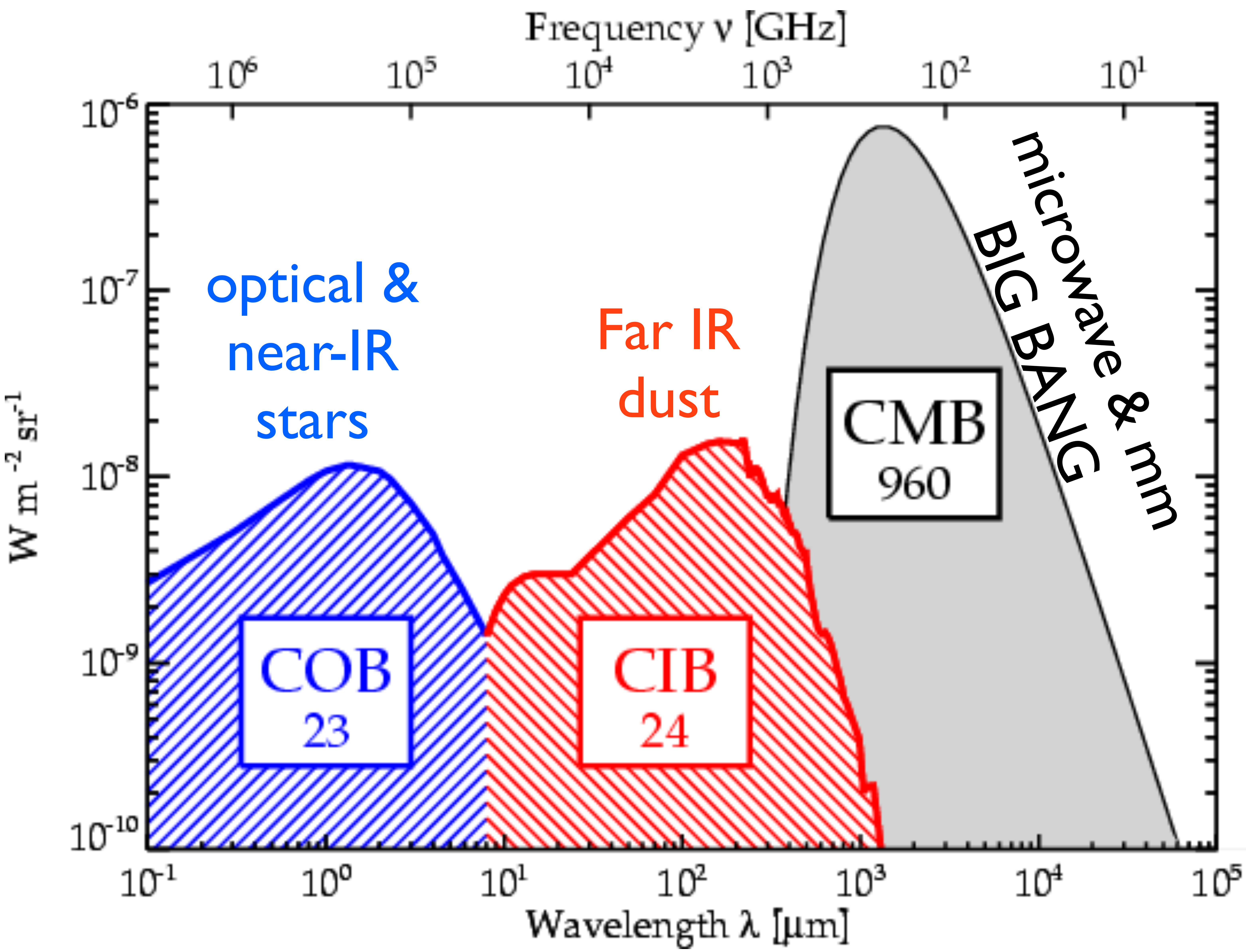


Dust emission is mostly reprocessed starlight: the radiation field warms the interstellar dust, which reradiates in the IR

# Galaxy tracks with redshift

Metcalfe et al. (1996)

FIG. 3 Dots represent the $U' - B' : B' - I'$ colours of galaxies with $B' < 27.5$ mag in the Hubble Deep Field. Primed letters for magnitudes indicate that here we are using the natural HST magnitude system, with the zero point set at an A0V star. The arrows represent detection upper limits, mainly galaxies which are undetected in $U'$. The $U' - B'$ colours move sharply redwards at $B' - I' \approx 0.8$ due to the Lyman-$\alpha$ forest/Lyman break passing through the $U'$ band. The predicted tracks are the $q_0 = 0.05$ evolutionary models for each morphological type as detailed in Fig. 1 legend, modulated in the case of Sbc/Scd/Sdm types by our assumed internal dust absorption of $A'_U = 0.45$ mag, $A'_B = 0.3$ mag, $A'_I = 0.11$ mag and in the case of all galaxies by the Lyman-$\alpha$ forest absorption. The models used in the $q_0 = 0.5$ case (not shown) show a very similar behaviour, even for the rapidly fading dE type. The $z = 1$ and $z = 2$ labelled positions on the tracks indicate the colours of model E/SO and Sdm galaxies at these redshifts. The remaining symbols show the colours of 45 brighter galaxies with Keck spectroscopic redshifts, and these agree well with the predicted colours for these galaxies. It can also be seen that $U' - B' < 0$ is predicted to correspond to galaxies with $z < 2$, and $U' - B' > 0$ to galaxies with $z > 2$.

Color-color plot with redshifted galaxy tracks

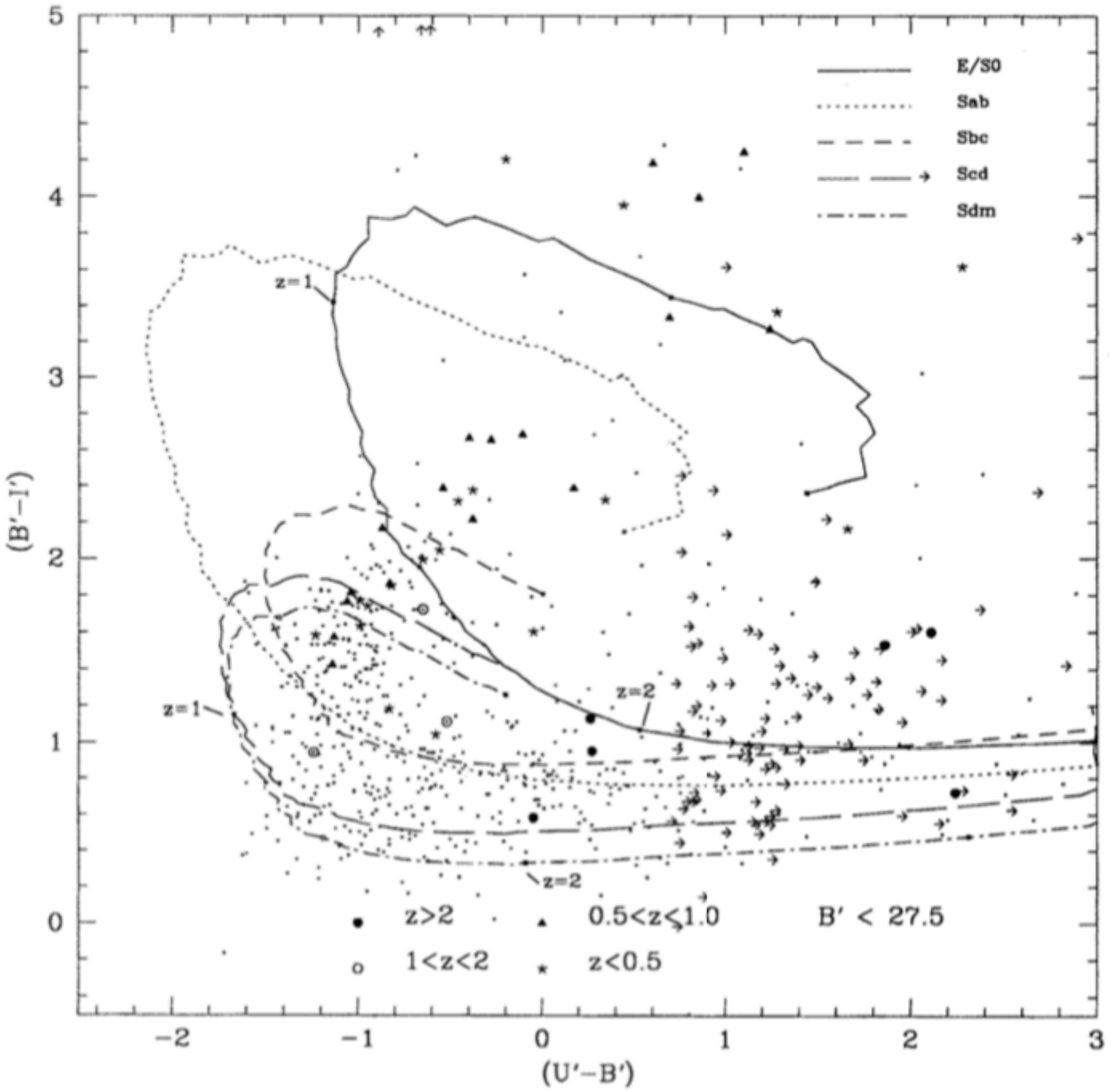

# K-corrections

A correction to the magnitude of an object to account for the redshifting of its spectrum $f(\lambda)$ through filter $S_i(\lambda)$

$$K(z,T) = -2.5\log\left[(1+z)\frac{\int_{\lambda_1}^{\lambda_2} S_i(\lambda)\, f(\lambda)\, d\lambda}{\int_{\lambda_1}^{\lambda_2} S_i(\lambda)\, f[\lambda(1+z)]\, d\lambda}\right]$$

spectral stretching

filter transmission window

change of spectrum through filter window

distance modulus becomes $$m_i - M_i = 5\log\left(\frac{D_L}{\text{Mpc}}\right) + 25 + A_i + K_i$$

specific to filter $i$

extinction

K-correction

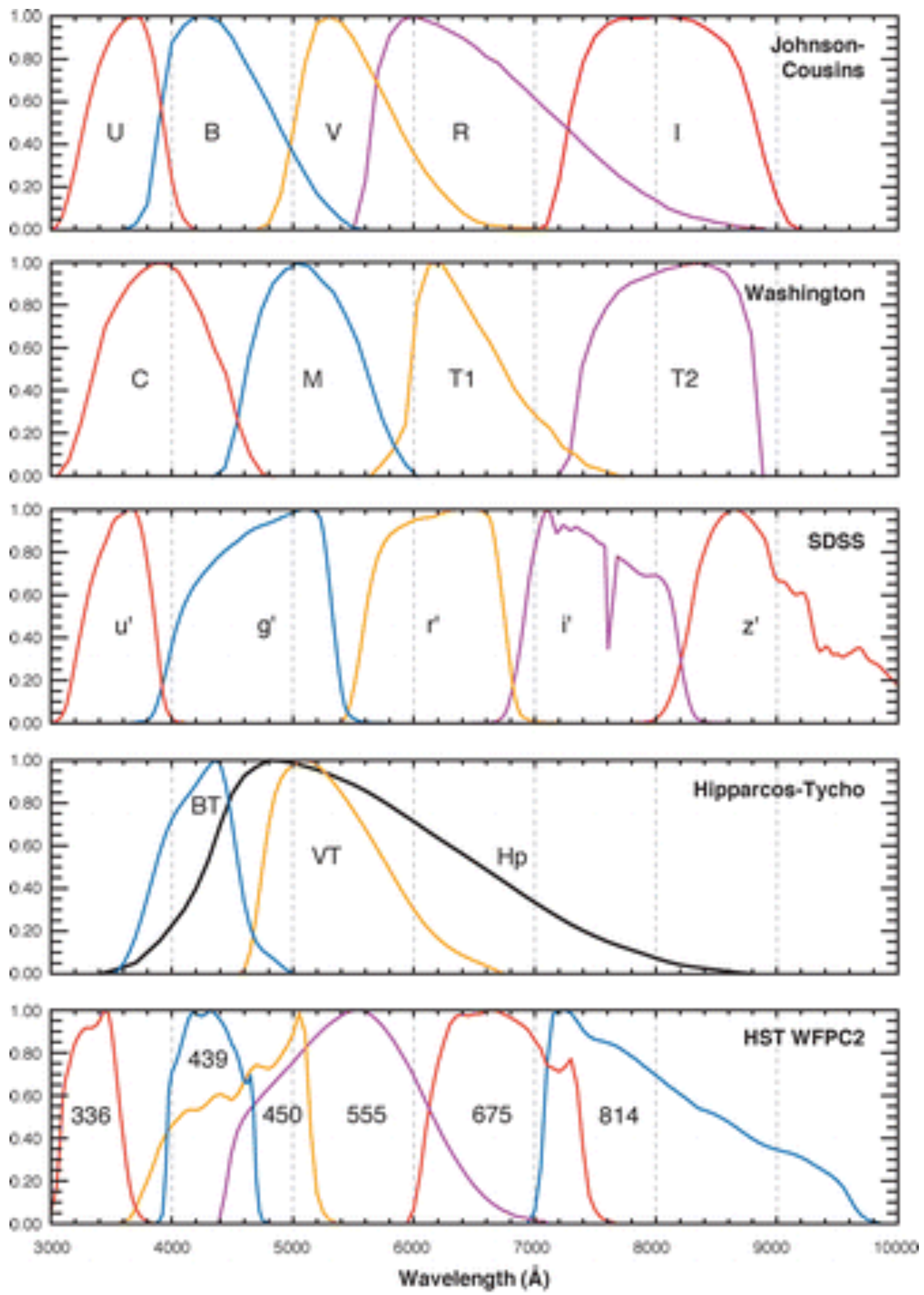


Bessell, MS. 2005
Annu. Rev. Astron. Astrophys. 43: 293–336

# K-corrections

$f(\lambda, T)$

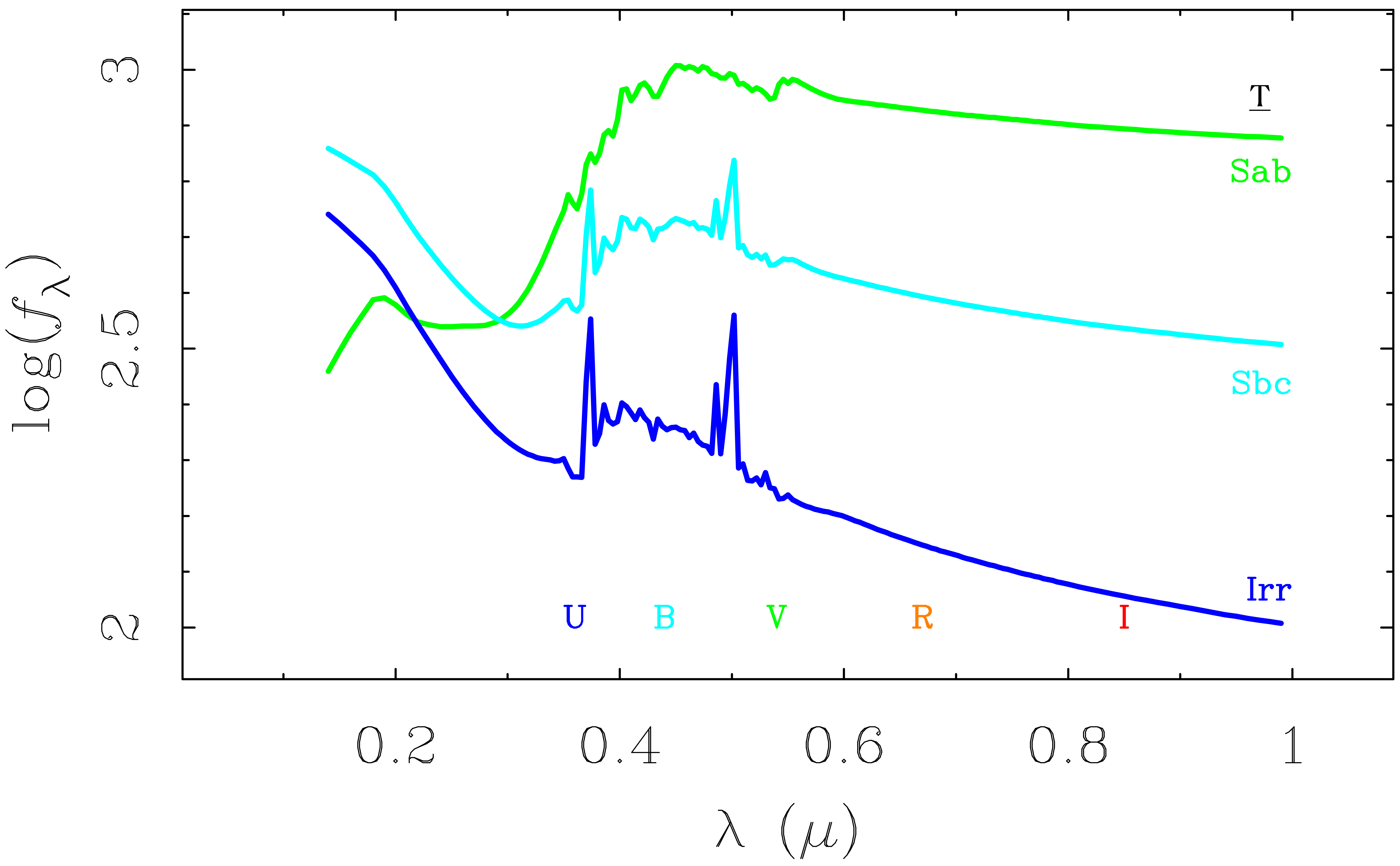

# K-corrections

Cosmic expansion causes the source spectrum to shift and stretch.

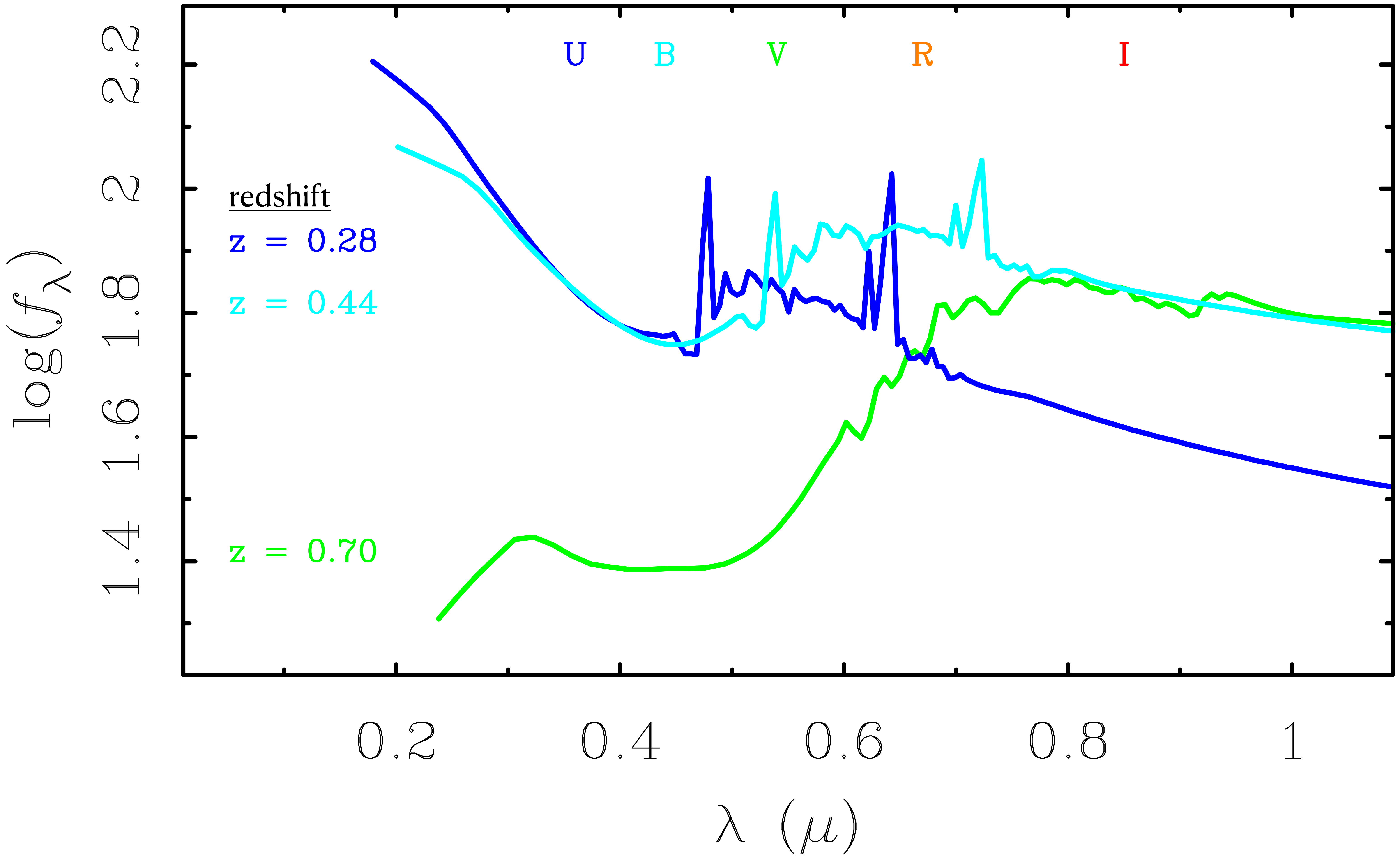


Any given filter provides a fixed window on the moving target of a redshifted spectrum. We observe a bluer part of the spectrum than that which was emitted in the rest frame of the filter.

# K-corrections

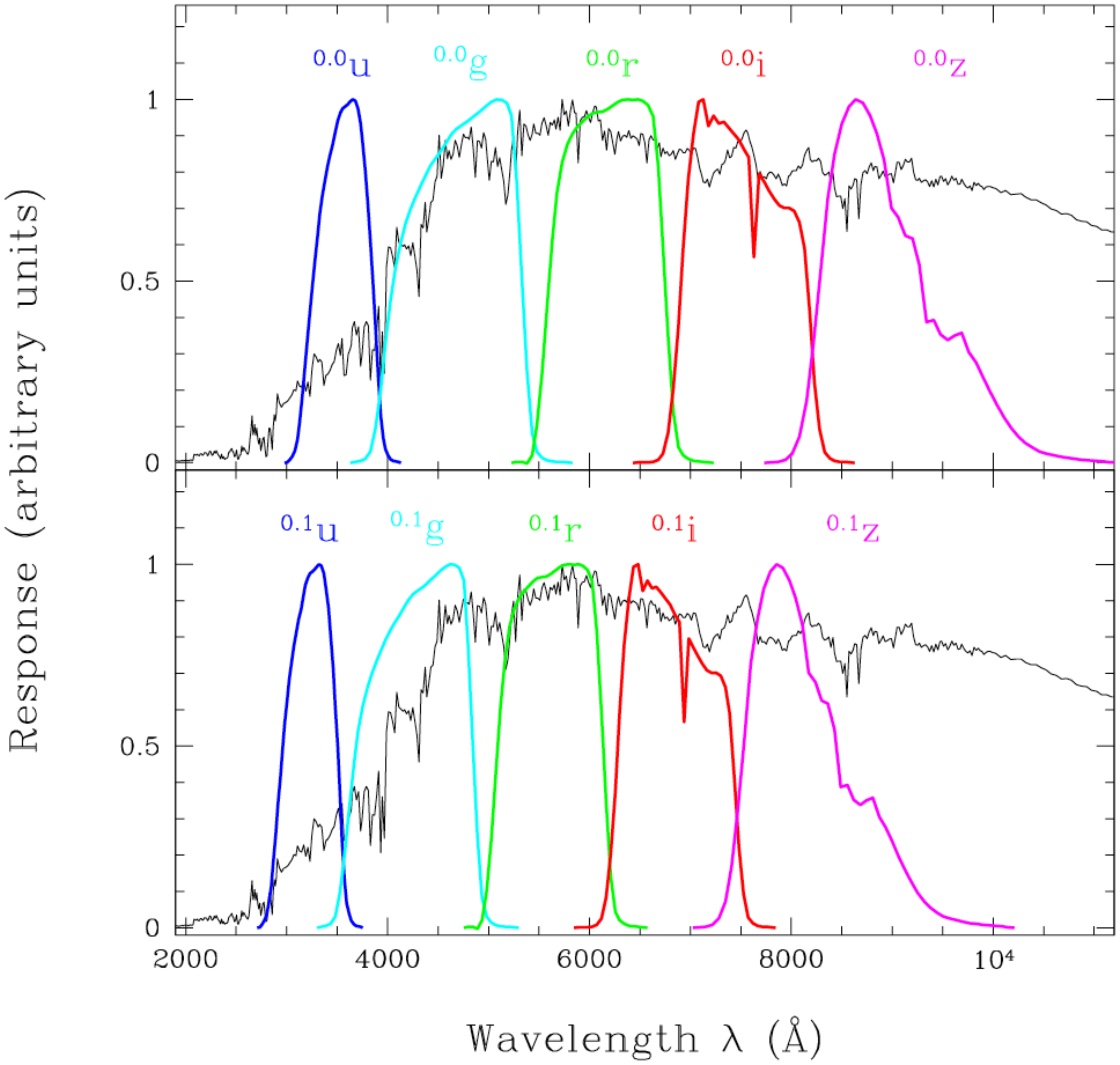


SDSS filters at z=0

SDSS filters at z=0.1

Blanton et al. (2002)

Fig. 2.— Demonstration of the differences between the unshifted SDSS filter system (0.0u , 0.0g , 0.0r , 0.0i , 0.0z ) in the top panel and the SDSS filter system shifted by 0. 1 (0.1u , 0.1g , 0.1r , 0.1i , 0.1z ) in the bottom panel. Shown for comparison is a 4 Gyr-old instantaneous burst population from an update of the Bruzual A. & Charlot (1993) stellar population synthesis models. The K -corrections between the magnitudes of a galaxy in the unshifted SDSS system observed at redshift z = 0. 1 and the magnitudes of that galaxy in the 0. 1-shifted SDSS system observed at redshift z = 0 are independent of the galaxy's spectral energy distribution (and for AB magnitudes are equal to − 2. 5 log10 (1 + 0. 1) for all bands; Blanton et al. 2002a). This independence on spectral type makes the 0. 1-shifted system a more appropriate system in which to express SDSS results, for which the median redshift is near redshift z = 0. 1.

# K-corrections

Lots and lots of filters minimizes the assumptions in $f(\lambda, T)$

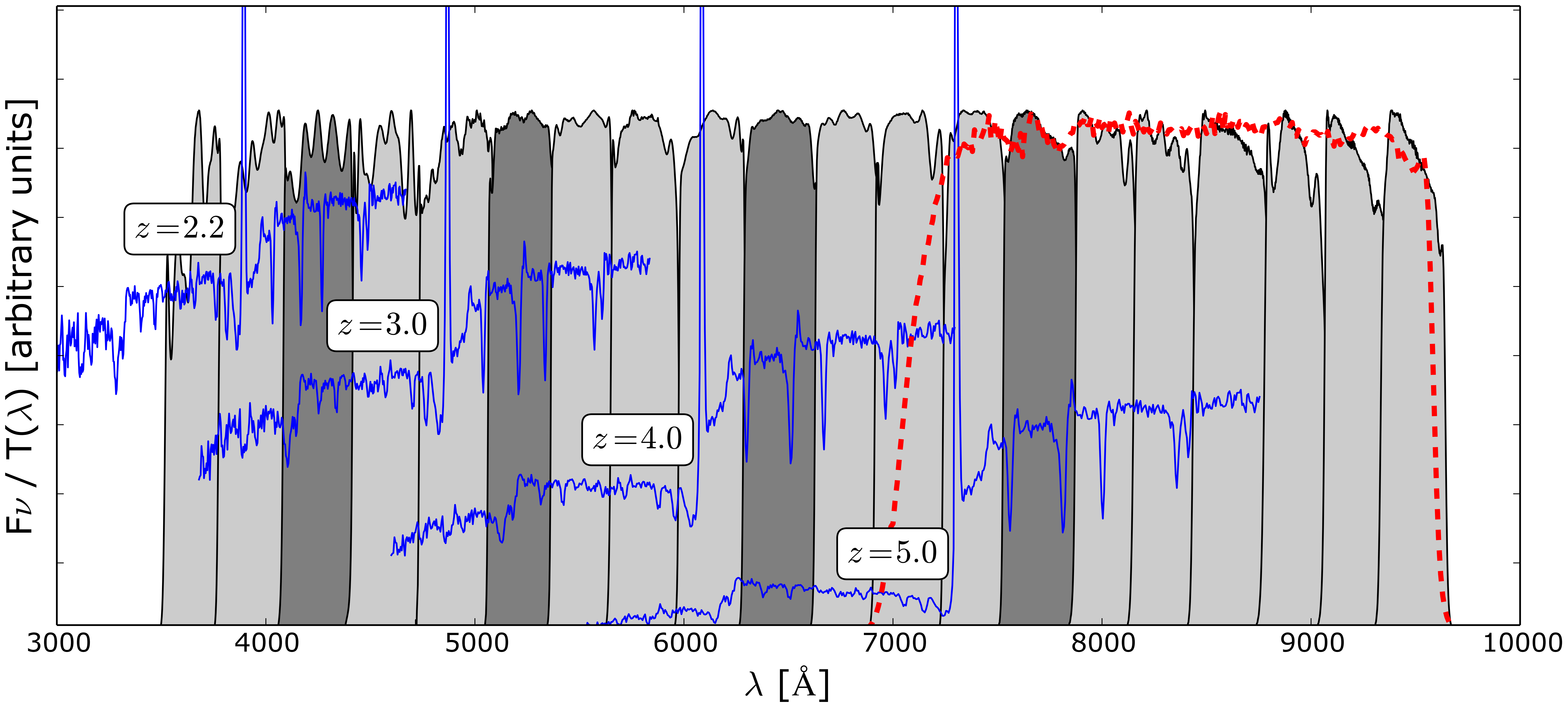

UV as it would appear in the HDF

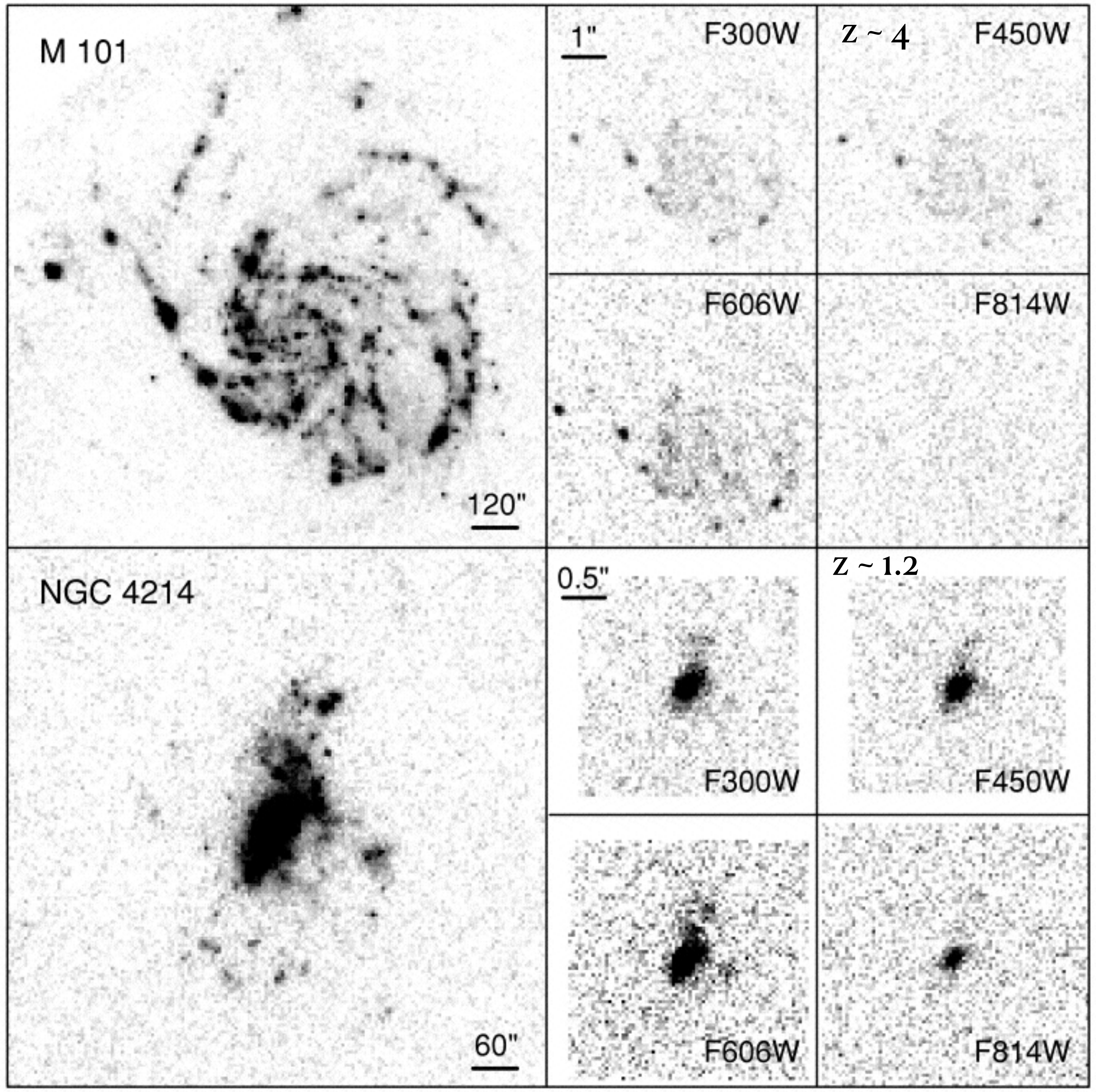


optical UV

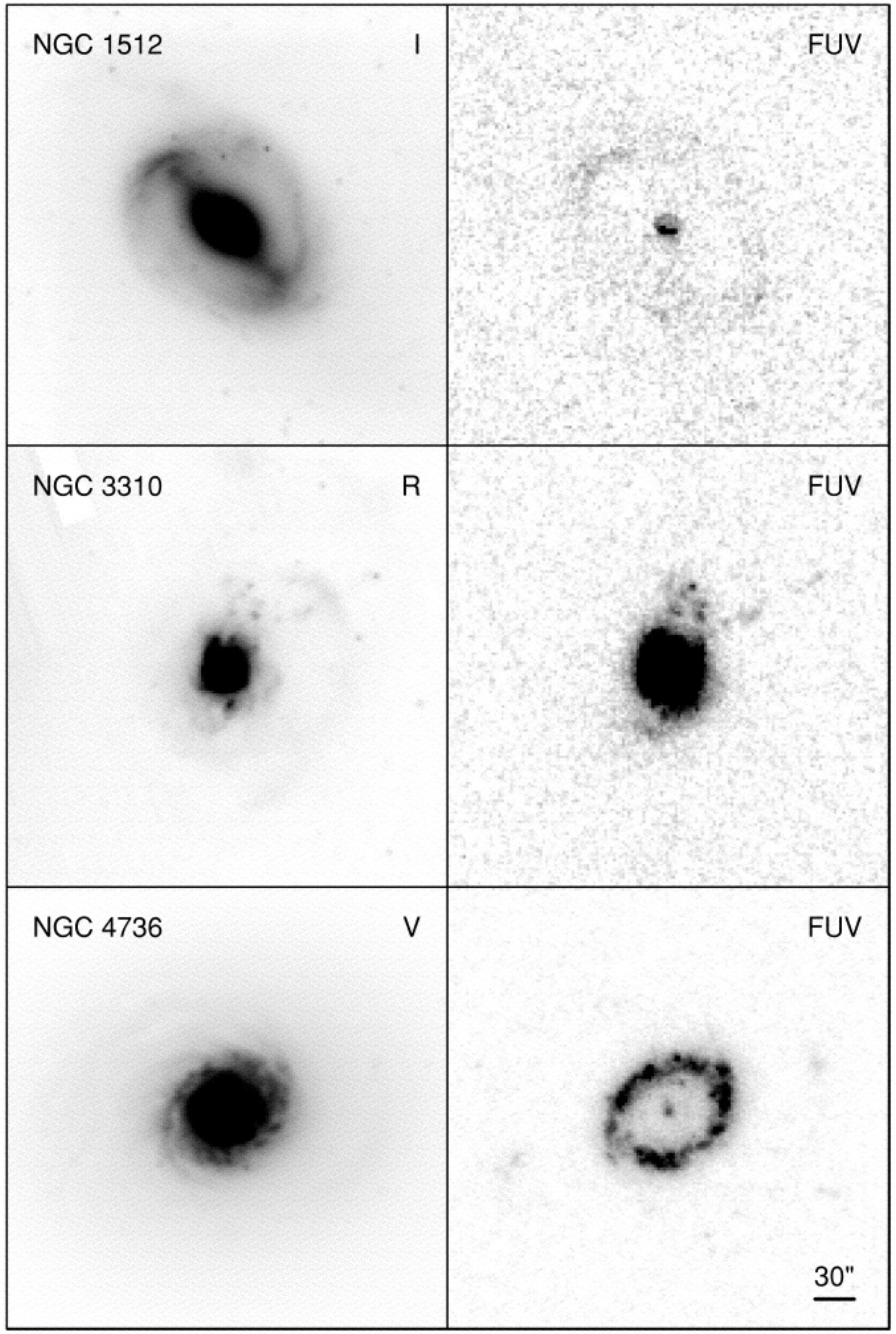


Kuchinski etal AJ 122 729

## Johnson filters UBVRI

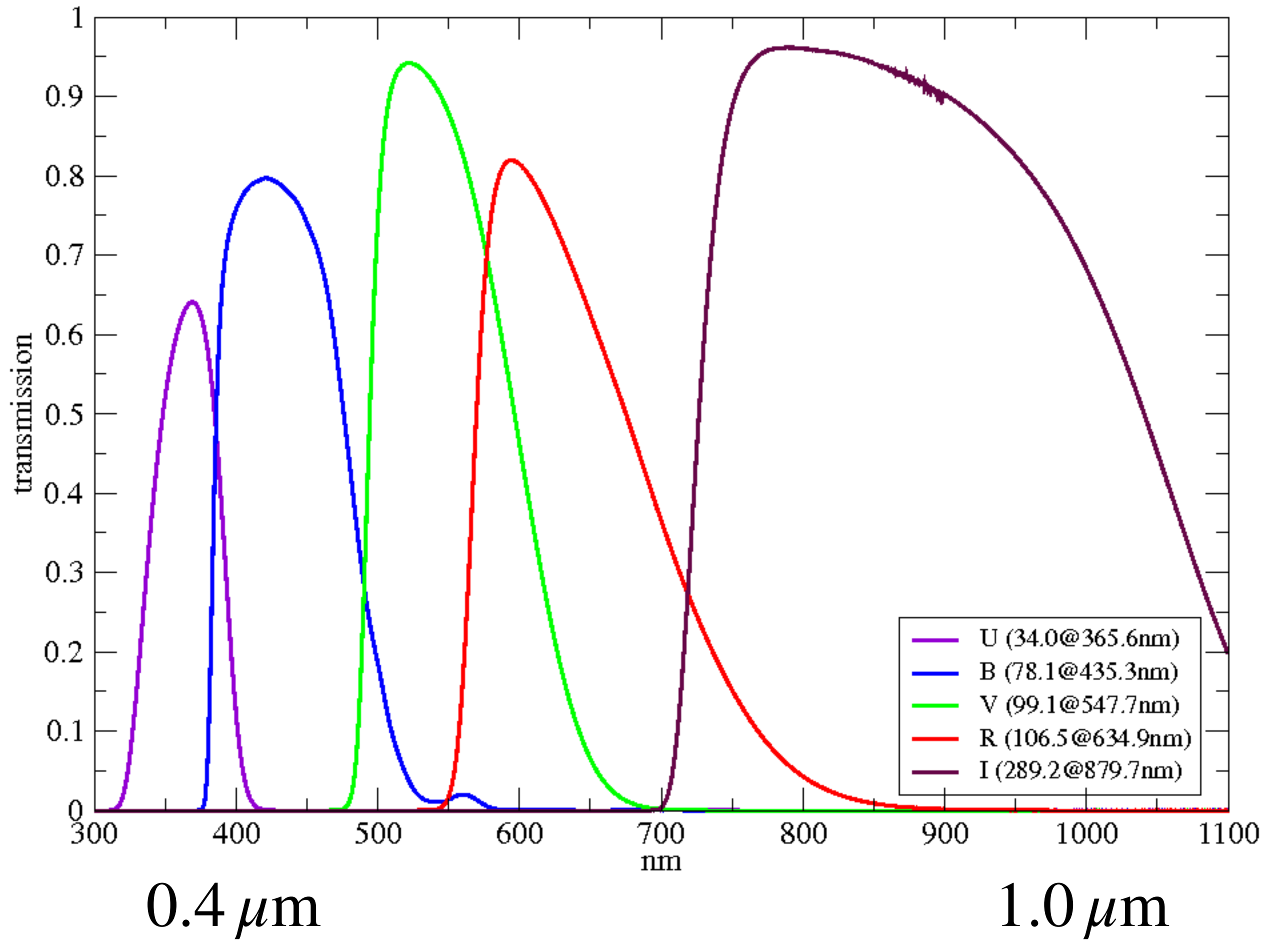


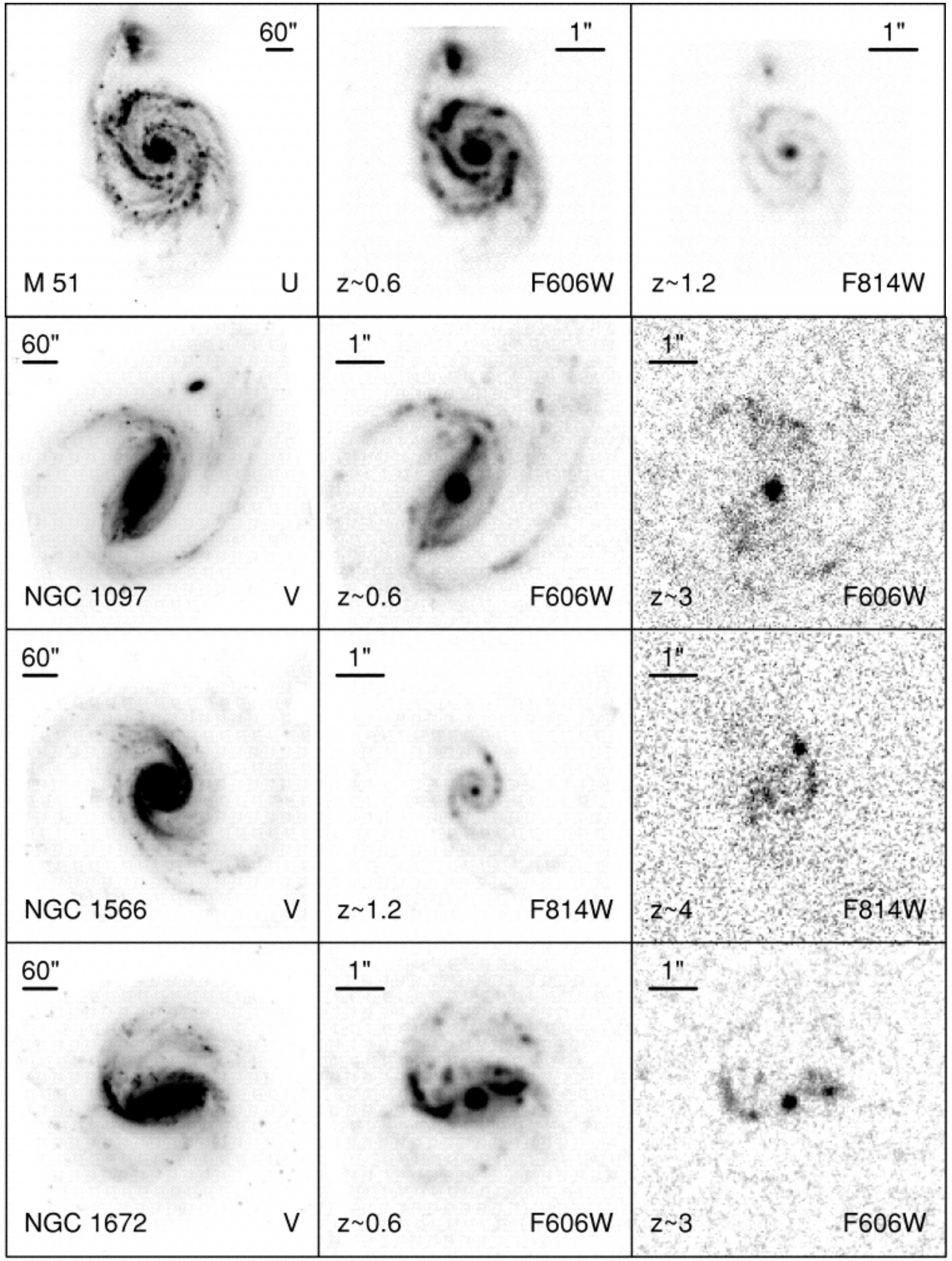


## HST/ACS and WFC3 filter set

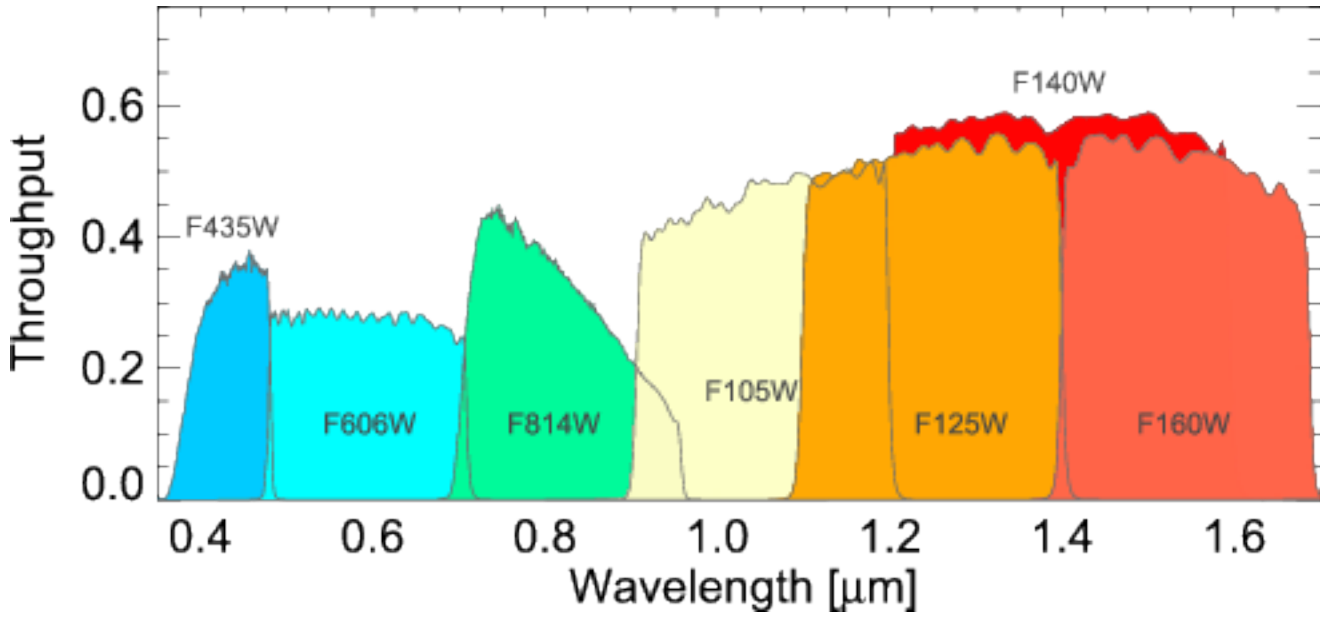


Kuchinski etal AJ 122 729

# Galaxy Evolution

Characteristic magnitude **m*** of protocluster galaxies as a function of redshift (**Franck 2017, Ph.D.**)

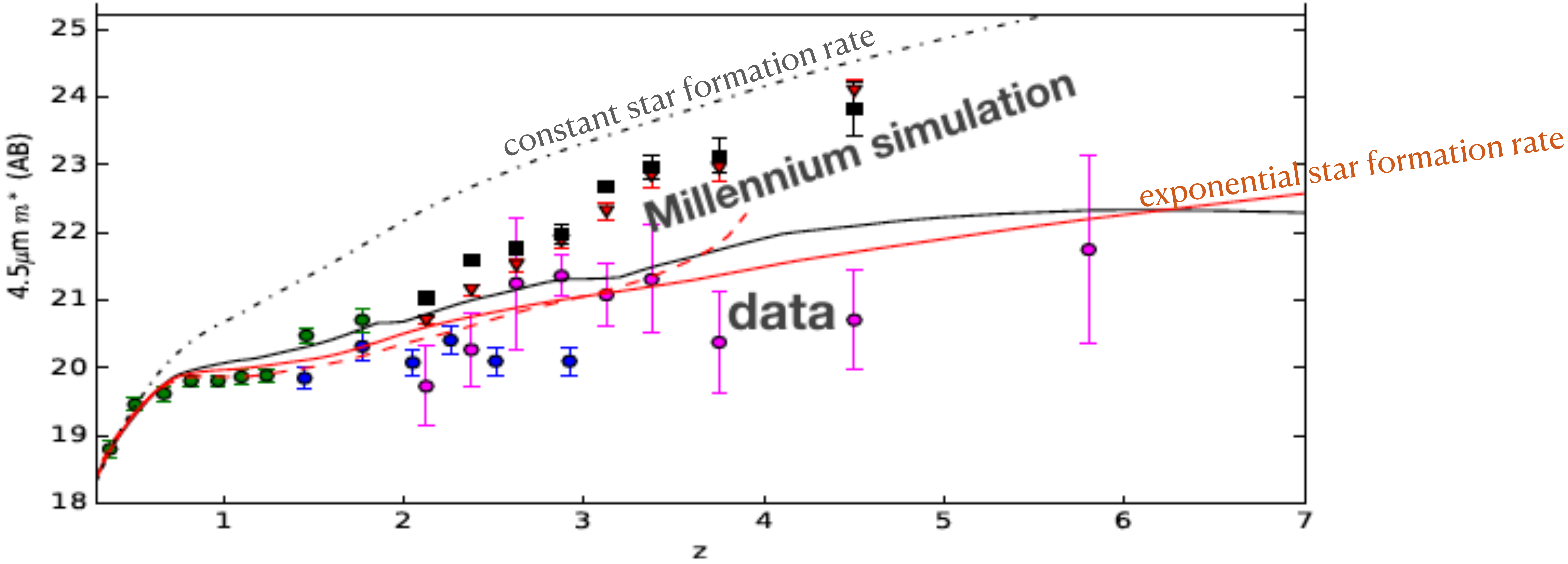


Galaxies are brighter and clustered sooner than predicted by LCDM simulations.

Since the volume depends on curvature, source counts provide a test

For sources of luminosities $L$ and constant comoving number density $\Phi(L)$,

Number-redshift:

$$N( < z) = \frac{4\pi}{3H_0^2} z^3 \int_0^\infty \Phi(L) \left[1 + \frac{3}{2} z(1 + q_0)\right] dL$$

Number-magnitude:

$$N( < f) = \frac{4\pi}{3} (4\pi f)^{-3/2} \int_0^\infty \Phi(L) \left[1 - 3H_0 \left(\frac{L}{4\pi f}\right)^{1/2}\right] L^{3/2} dL$$

# Number-redshift:

Metcalfe et al. (1996)

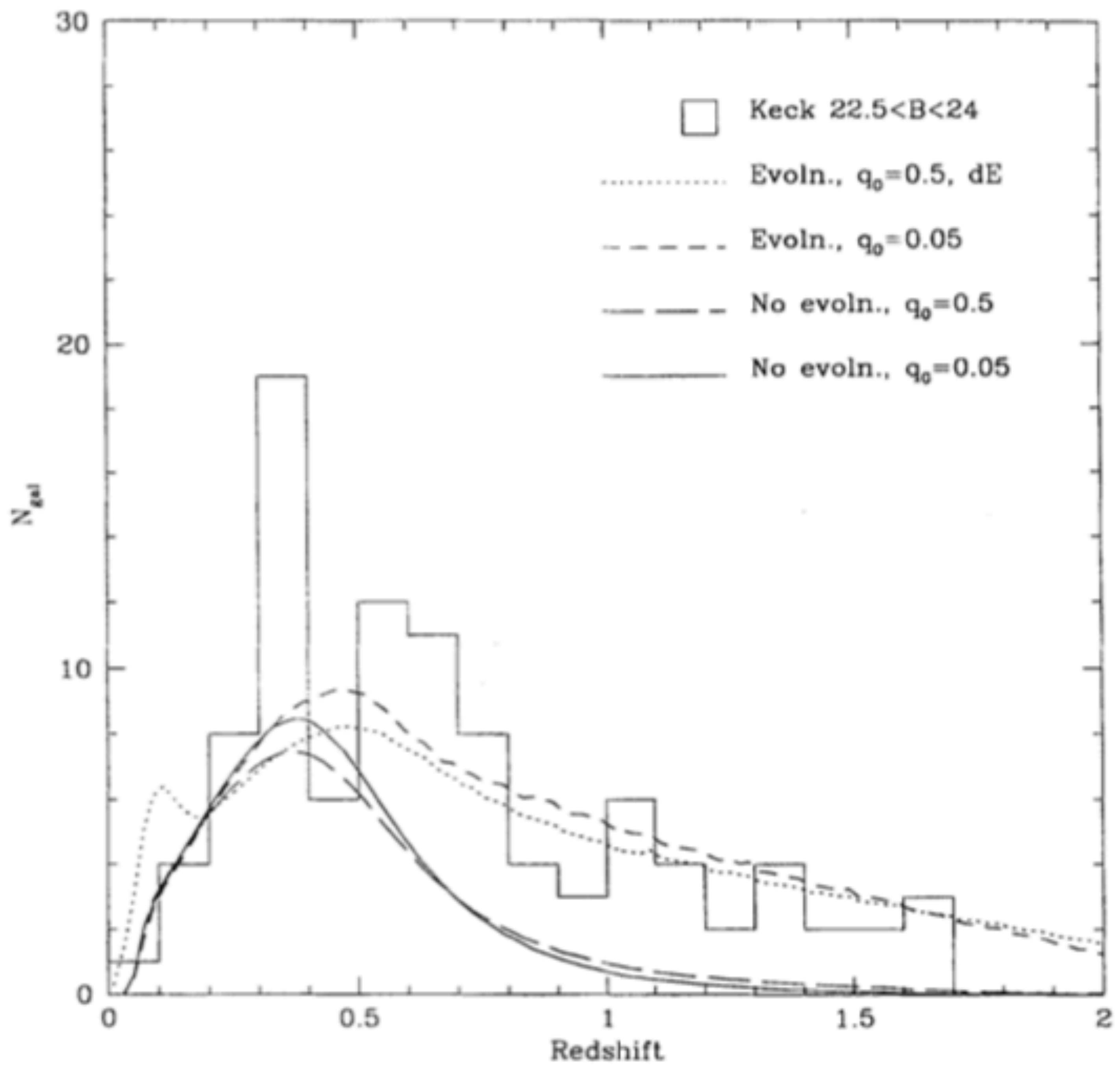


FIG. 2 The galaxy number–redshift distribution, $n(z)$, for $22.5\,\mathrm{mag} < B < 24\,\mathrm{mag}$ implied by new redshift data acquired on the Keck Telescope (refs. 6, 7). The observed $n(z)$ is clearly more extended than the non-evolving models with either $q_0 = 0.05$ or $q_0 = 0.5$. The extended redshift distribution is well fitted by our evolutionary models whose parameters are described in Fig. 1 legend.

Large Scale Structure is apparent in the non-smoothness of N(z).

Galaxies evolve!

Certainly in luminosity,
probably also in number.

So a single Schechter fcn doesn't suffice.
All of these terms matter.

$$A(m,T) = A_0 \int_0^z D(z,T)\Phi(M,T)dV(z,q_0)$$

Density distribution (e.g., non-uniform large scale structure)

Luminosity function n(L)↔Φ(M)

Volume element (cosmological)

## Number-redshift:

Franck & McGaugh (2016)

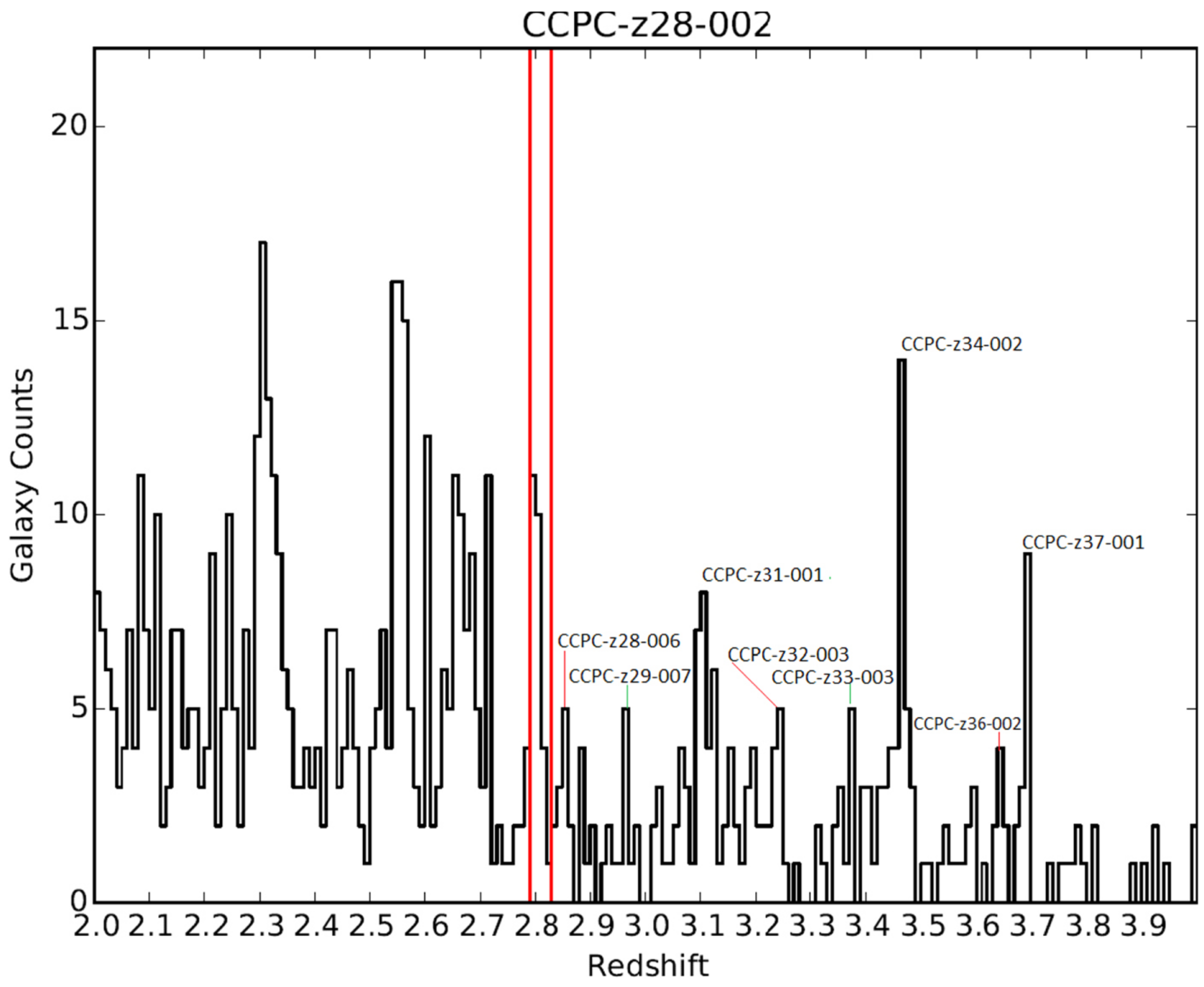


Large Scale Structure is apparent in the non-smoothness of N(z).

Galaxies evolve!
Certainly in luminosity,
probably also in number.

So a single Schechter fcn doesn't suffice.
All of these terms matter.

$$A(m,T) = A_0 \int_0^z D(z,T)\Phi(M,T)dV(z,q_0)$$

Density distribution (e.g., non-uniform large scale structure)

Luminosity function $n(L) \leftrightarrow \Phi(M)$

Volume element (cosmological)

Unexpected structure in N(z) persists to high redshift: the density distribution D(z,T) is non-uniform (red lines indicate one of many candidate proto-galaxy clusters (named).